

Multiscale modeling of fiber reinforced materials via non-matching immersed methods

Giovanni Alzetta^a, Luca Heltai^a

^a*SISSA-International School for Advanced Studies
via Bonomea 265, 34136 Trieste - Italy*

Abstract

Fiber reinforced materials (FRMs) can be modeled as bi-phasic materials, where different constitutive behaviors are associated with different phases. The numerical study of FRMs through a full geometrical resolution of the two phases is often computationally infeasible, and therefore most works on the subject resort to homogenization theory, and exploit strong regularity assumptions on the fibers distribution. Both approaches fall short in intermediate regimes where lack of regularity does not justify a homogenized approach, and when the fiber geometry or their numerosity render the fully resolved problem numerically intractable.

In this paper, we propose a distributed Lagrange multiplier approach, where the effect of the fibers is superimposed on a background isotropic material through an independent description of the fibers. The two phases are coupled through a constraint condition, opening the way for intricate fiber-bulk couplings as well as allowing complex geometries with no alignment requirements between the discretisation of the background elastic matrix and the fibers.

We analyze both a full order coupling, where the elastic matrix is coupled with fibers that have a finite thickness, as well as a reduced order model, where the position of their centerline uniquely determines the fibers. Well posedness, existence, and uniqueness of solutions are shown both for the continuous models, and for the finite element discretizations. We validate our approach against the models derived by the rule of mixtures, and by the Halpin-Tsai formulation.

Keywords: Immersed boundary method, finite element method, fiber composites, Lagrange multipliers

1. Introduction

Numerous engineering applications require the efficient solution of partial differential equations involving multiple, complex geometries on different phases; *composite materials* are the prototypical example of such problems. During the past fifty years, the interest

Email addresses: giovanni.alzetta@sissa.it (Giovanni Alzetta), luca.heltai@sissa.it (Luca Heltai)

in composite materials flourished multiple times; it began for their applications to new materials in multiple fields, such as aerospace engineering [21], civil engineering [42], and materials science [7, 40].

During the nineties, the increasing importance of biomechanics in life sciences lead to the development of numerous models describing, e.g., arterial walls [29], soft tissues [27], and muscle fibers [30].

Recent years saw the rise of new application fields, such as the study of natural fiber composites [48], and engineering methods to accurately recover the three-dimensional structure of a material sample, e.g., [31, 32].

From the first studies on composites, it has been clear that their properties are strongly dependent on their internal structure: the volume ratio between each component, the orientation, the shape, all contribute substantially to the material's properties [21, 22]. One of the most wide-spread and significant example of composites is that of Fiber Reinforced Materials (FRMs), where thin, elongated structures (the fibers) are immersed in an underlying isotropic material (the elastic matrix).

We may separate the approaches used to study FRMs into two broad groups: i) “*homogenization methods*”, which study a complex inhomogeneous body by approximating it with a fictitious homogeneous body that behaves globally in the same way [55], and ii) “*fully resolved*” methods, which use separate geometrical and constitutive descriptions for the elastic matrix and the individual fibers.

As examples of analytical “*homogenization methods*” we recall the rule of mixtures [20] and the *empirical* Halpin-Tsai equations [19], used to study a transversely isotropic unidirectional composite, where fibers are uniformly distributed and share the same orientation. The development of homogenization theory led, in recent years, to more complex models, e.g., [28, 6].

More intricate homogenization approaches rely on numerical methods to provide a “cell” behaviour, which is then replicated using periodicity, using, e.g., the Finite Element Method [1, 45, 37], Fourier transforms [43, 44, 17], or Stochastic Methods [38].

The fundamental limit of all “*homogenization methods*” approaches is the impossibility of adapting them to study composites with little regularity. In these cases, the different phases are typically modeled separately, as a continuum. This approach began with Pipkin [49] on two dimensional membranes, and was then expanded to three dimensional examples by others (see, e.g., [34] for a detailed bibliography).

Fully resolved methods allow richer structures, but require a high numerical resolution, especially when material phases have different scales. The complex meshing and coupling often result in an unbearable computational cost, limiting the use of these methods.

The purpose of this paper is to introduce a new approach which is fit for materials that have *intermediate* properties, i.e., they possess no particular regularity, and are made by a relatively high number of fiber components. We propose an FRMs model inspired by the Immersed Boundary Method (IBM) [47], and by its variational counterparts [11, 23, 25, 51, 26], where the elastic matrix and the fibers are modeled independently, and coupled through a non-slip condition. We aim at providing an efficient numerical method for FRMs that allows the modeling of complex networks of fibers, where one may also be interested in the elastic properties of single fibers, without requiring the resolution of the single fibers in the background elastic matrix. From the computational point of view, this approach allows the use of two independent discretizations: one describing the

fibers, and one describing the *whole domain*, i.e., both the elastic matrix and the fibers. A distributed Lagrange multiplier is used to couple the independent grids, following the same spirit of the finite element immersed boundary method [9, 11], separating the Cauchy stress of the whole material into a background uniform behavior and a *excess* elastic behavior on the fibers.

Section 2 introduces the classical fully resolved model of a collection of fibers immersed in an elastic matrix. For simplicity, we do not include dissipative terms, and restrict our study to linearly elastic materials. The problem is then reformulated exploiting classical results of mixed methods (see Chapter 4 of [8]), following ideas similar to those found in [10], proving that both the continuous and discrete formulations we propose are well-posed with a unique solution.

The use of a full three dimensional model for the fibers still results in high computational costs; the obvious simplification would be to approximate the fibers with one-dimensional structures. This approach is non-trivial because it is not possible to consider the restriction of a Sobolev function defined on a three-dimensional domain to a one-dimensional domain. A possible solution involves the use of weighted Sobolev spaces, combined with graded meshes [15, 14] but, if the number of fibers is large, graded meshes may still be too computationally intensive. In Section 3, we propose and analyze an alternative solution, where additional modellistic assumptions enable a $3D - 1D$ coupling that relies on local averaging techniques. A similar procedure is used in [24] to model vascularized tissues. To conclude, we validate our thin fiber model in Section 4, and draw some conclusions in Section 5.

2. Three-dimensional model

Many bi-phasic materials present a relatively simple fiber structure but result in a very intricate elastic matrix. Consider, for example, Figure 1: constructing a discretization grid for the fibers themselves maybe simple enough, but building a fully resolved grid for the *surrounding* elastic matrix, in this case, may require excessive resolution, and result in a computationally hard problem to solve. We wish to describe a new approach, where we substitute the complex mesh needed for the elastic matrix with a simple one describing the whole domain, and overlap the fiber structure independently with respect to the background grid, and couple the two systems via distributed Lagrange multipliers.

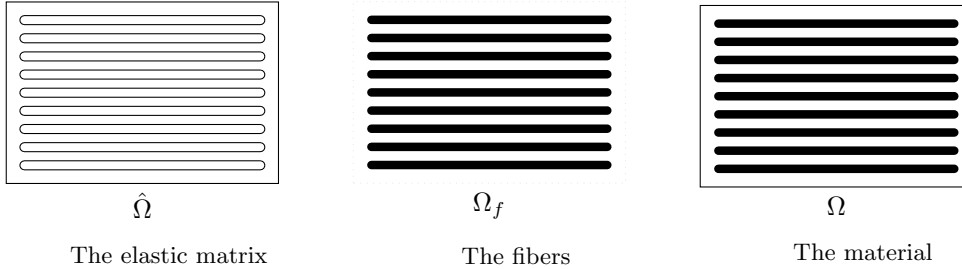
2.1. Problem formulation

As a model bi-phasic material, we consider a linearly elastic fiber reinforced material. To simplify the treatment of the problem, in this work we limit ourselves to the quasi-static small strain regime. The extension to finite strain elasticity and dynamic problems does not present additional difficulties and is going to be the subject of a future work.

To describe the composite, we use a connected, bounded, Lipschitz domain $\Omega \subset \mathbb{R}^d$ of dimension $d = 3$, composed of a fiber phase $\Omega_f \subset \Omega$, and an elastic matrix $\hat{\Omega} := \Omega \setminus \Omega_f \subset \mathbb{R}^d$, which we assume to be a connected, Lipschitz domain. We describe each of the $n_f \in \mathbb{N}$ fibers with a connected, Lipschitz domain and Ω_f is obtained as the union of these (possibly overlapping) domains.



Figure 1: An example of a fiber structure for which the mesh generation for the fibers would be trivial, but the resulting three-dimensional elastic matrix would be much more expensive to resolve in full.



Example of a two-dimensional section of an FRM with uniformly oriented fibers.

Remark. *The results of this section hold for a general domain Ω_f , union of multiple components with the required regularity. The property of the fibers of being thin, elongated, structures, is only needed for the model of Section 3, and plays no role in this Section.*

Given a displacement field $u: \Omega \rightarrow \mathbb{R}^d$, representing a deformation from the equilibrium configuration, the corresponding stress tensor on Ω can be expressed using the stress-strain law [18]:

$$S[u] = \mathbb{C}\nabla u,$$

where \mathbb{C} is a symmetric 4th order tensor that takes the form:

$$\mathbb{C} = \begin{cases} \mathbb{C}_\Omega & \text{in } \hat{\Omega}, \\ \mathbb{C}_f & \text{in } \Omega_f. \end{cases} \quad (1)$$

Here \mathbb{C}_Ω and \mathbb{C}_f are assumed to be constant over their respective domains, and represent the elasticity tensors of the elastic matrix and of the fibers. The classical formulation of static linear elasticity can be thought of as a force balance equation (see, for example, [18]):

Problem 1 (Classic Strong Formulation). *Given an external force density field b , find the displacement u such that*

$$\begin{aligned} -\operatorname{div}(\mathbb{C}u) &= b && \text{in } \Omega, \\ u &= 0 && \text{on } \partial\Omega. \end{aligned} \quad (2)$$

Due to the piecewise nature of \mathbb{C} , it is natural to reformulate Problem 1 into a variational or weak formulation. Given a subset D of $\partial\Omega$, we introduce the notation for the subspace of the Sobolev space $H^1(\Omega)$ with functions vanishing on a subset D of the boundary $\partial\Omega$:

$$H_{0,D}^1(\Omega)^d := \{v \in H^1(\Omega)^d: v|_D = 0\},$$

with norm $\|\cdot\|_V = \|\cdot\|_{H^1(\Omega)} := \|\cdot\|_\Omega + \|\nabla \cdot\|_\Omega$, where the symbol $\|\cdot\|_A$ represents the $L^2(A)$ norm over the measurable set $A \subset \Omega$, and $(\cdot, \cdot)_A$ represents the L^2 scalar product on the given domain A . We define the following space:

$$V := (H_{0,\partial\Omega}^1(\Omega))^d = \{v \in H^1(\Omega)^d: v|_{\partial\Omega} = 0\},$$

The standard weak formulation reads:

Problem 2 (Classic Weak Formulation). *Given $b \in L^2(\Omega)^d$, find $u \in V$ such that:*

$$(\mathbb{C}\nabla u, \nabla v)_\Omega = (b, v)_\Omega \quad \forall v \in V. \quad (3)$$

The main idea behind our reformulation is to rewrite Problem 2 into an equivalent form, where we define two independent functional spaces. The novelty we introduce is to define the functional spaces on Ω and Ω_f , and not on $\hat{\Omega}$ and Ω_f . To achieved this, we define two fictitious materials: one with the same properties of the elastic matrix, occupying the full space Ω , and one describing the “excess elasticity” of the fibers separately, defined on Ω_f only. The first step in this direction is to split the left-hand side of Equation 3 on the two domains:

$$\begin{aligned} (\mathbb{C}\nabla u, \nabla v)_\Omega &= (\mathbb{C}_f \nabla u, \nabla v)_{\Omega_f} + (\mathbb{C}_\Omega \nabla u, \nabla v)_{\hat{\Omega}} \\ &= (\mathbb{C}_f \nabla u, \nabla v)_{\Omega_f} + \underbrace{(\mathbb{C}_\Omega \nabla u, \nabla v)_{\hat{\Omega}} + (\mathbb{C}_\Omega \nabla u, \nabla v)_{\Omega_f}}_{\Omega} - (\mathbb{C}_\Omega \nabla u, \nabla v)_{\Omega_f} \\ &= (\mathbb{C}_\Omega \nabla u, \nabla v)_\Omega + (\delta \mathbb{C}_f \nabla u, \nabla v)_{\Omega_f}, \end{aligned}$$

where $\delta \mathbb{C}_f := \mathbb{C}_f - (\mathbb{C}_\Omega)|_{\Omega_f}$.

For simplicity, we improperly use the expression “elastic matrix equation” and “fiber equation”, even though they should be really considered as the “whole domain equation”, and a “delta fiber equation”.

This formal separation does not change the original variational problem, which can still be stated explicitly: given $b \in L^2(\Omega)^d$, find $u \in V$ such that:

$$(\mathbb{C}_\Omega \nabla u, \nabla v)_\Omega + (\delta \mathbb{C}_f \nabla u, \nabla v)_{\Omega_f} = (b, v)_\Omega \quad \forall v \in V. \quad (4)$$

To simplify the coupling between the fibers and the elastic matrix, we need to split Equation 4 on two functional spaces, describing their boundary conditions.

The boundary of the domain Ω induces a natural splitting on the boundary of the fibers: we define the following partition of $\partial\Omega_f$:

$$B_i := \partial\Omega_f \setminus \partial\Omega \quad (5)$$

$$B_e := \partial\Omega \cap \partial\Omega_f, \quad (6)$$

where B_i is the interface between the fibers and the elastic matrix, while B_e is the interface between the fibers the exterior part of Ω , that lies on the boundary $\partial\Omega$.

Next we define the restriction of $H_0^1(\Omega)$ on the fibers:

$$W := (H_{0, B_e}^1(\Omega_f))^d. \quad (7)$$

With the explicit introduction of the space W we can modify Problem 2 by separating the solution into two components, one describing the whole matrix, the other describing the fibers.

To achieve this we introduce a non-slip condition coming some well-known properties of FRMs (for more details see, e.g., [13], Chapter 16); the mechanical characteristics of a FRM do not depend only on the properties of the two phase materials, but also on the degree to which an applied load is transmitted from the elastic matrix to the fiber. The transmission depends on:

- The fiber-matrix bond strength τ_c , i.e., the degree to which an applied load is transmitted to the fibers through the interfacial bond between the fiber and the matrix phases.
- The fiber length, because the matrix-fiber bond greatly reduces at the extremities.

The fact that, at the edges of the fiber, the load transmittance reduces, leads to the definition of a **critical fiber length** l_c , dependent on both the fiber radius a and τ_c :

$$l_c \propto \frac{a}{\tau_c}.$$

If the fibers are shorter than this critical value l_c , the stress transference becomes negligible, while longer fibers generally result in better reinforcement for the material [13]. Fibers for which the length l is $l \gg l_c$ are called **continuous fibers**.

To simplify our model we consider continuous fibers with a “perfect bond” between the two phases, leading to the same deformation of both materials. Mathematically, the bond is imposed through an interface condition: the following **non-slip** constraint for the solution $(u, w) \in V \times W$:

$$u|_{\Omega_f} = w. \quad (8)$$

To easily the continuity at the boundary of the two components and Equation 8, one should choose matching grids for Ω and Γ . To avoid this inconvenience we follow the distributed Lagrange multiplier approach described in [9, 4, 12].

The modified problem can be described as a constrained minimization problem:

$$u, w = \arg \inf_{\substack{u \in V \\ w \in W \\ \text{subject to} \\ u|_{\Omega_f} = w}} \psi(u, w), \quad (9)$$

where we defined the total elastic energy of the system as

$$\psi(u, w) = \frac{1}{2}(\mathbb{C}_\Omega \nabla u, \nabla u)_\Omega + \frac{1}{2}(\delta \mathbb{C}_f \nabla w, \nabla w)_{\Omega_f} - (b, u)_\Omega. \quad (10)$$

To impose the non-slip constraint of Equation 8 in weak form, several choices are possible. One may use, for example, the scalar product of W , or the duality product $W' \times W$ as in [10]. In this work, we use the latter, with $Q := H^{-1}(\Omega_f)^d$, which enforces the transmission condition on the interface (see [4, 12]):

$$\langle q, u|_{\Omega_f} - w \rangle_{Q \times W} = 0 \quad \forall q \in Q. \quad (11)$$

For simplicity we shall avoid the subscript $Q \times W$ from now on.

The constrained minimization expressed in Equation 9 is equivalent to the saddle point problem:

$$u, w, \lambda = \arg \inf_{\substack{u \in V \\ w \in W}} \left(\arg \sup_{\lambda \in Q} \psi(u, w, \lambda) \right), \quad (12)$$

where the constraint is imposed weakly as in 11 with a Lagrange multiplier:

$$\psi(u, w, \lambda) := \frac{1}{2}(\mathbb{C}_\Omega \nabla u, \nabla u)_\Omega + \frac{1}{2}(\delta \mathbb{C}_f \nabla w, \nabla w)_{\Omega_f} + \langle \lambda, u|_{\Omega_f} - w \rangle - (b, u)_\Omega.$$

A solution to Equation 12 is obtained by solving the Euler-Lagrange equation:

$$\langle D_u \psi, v \rangle + \langle D_w \psi, y \rangle + \langle D_\lambda \psi, q \rangle = 0 \quad \forall v \in V, \forall y \in W, \forall q \in Q, \quad (13)$$

that is:

Problem 3 (Saddle Point Weak Formulation). *Given $b \in L^2(\Omega)^d$, find $u \in V, w \in W, \lambda \in Q$ such that:*

$$(\mathbb{C}_\Omega \nabla u, \nabla v)_\Omega + \langle \lambda, v|_{\Omega_f} \rangle = (b, v)_\Omega \quad \forall v \in V \quad (14)$$

$$(\delta \mathbb{C}_f \nabla w, \nabla y)_{\Omega_f} - \langle \lambda, y \rangle = 0 \quad \forall y \in W \quad (15)$$

$$\langle q, u|_{\Omega_f} - w \rangle = 0 \quad \forall q \in Q, \quad (16)$$

or, equivalently,

$$\begin{array}{llll} \mathcal{K}_\Omega u & + \mathcal{B}^T \lambda & = (b, \cdot)_\Omega & \text{in } V' \\ & \mathcal{K}_f w & - \mathcal{M}^T \lambda & = 0 & \text{in } W' \\ \mathcal{B} u & - \mathcal{M} w & = 0 & \text{in } Q', \end{array} \quad (17)$$

where

$$\begin{array}{ll} \mathcal{K}_\Omega: V \rightarrow V' & \langle \mathcal{K}_\Omega u, \cdot \rangle := (\mathbb{C}_\Omega \nabla u, \nabla \cdot)_\Omega \\ \mathcal{K}_f: W \rightarrow W' & \langle \mathcal{K}_f w, \cdot \rangle := (\delta \mathbb{C}_f \nabla w, \nabla \cdot)_{\Omega_f} \\ \mathcal{B}: V \rightarrow Q' & \langle \mathcal{B} u, \cdot \rangle := \langle \cdot, u|_{\Omega_f} \rangle \\ \mathcal{M}: W \rightarrow Q' & \langle \mathcal{M} w, \cdot \rangle := \langle \cdot, w \rangle. \end{array} \quad (18)$$

2.2. Well-posedness, existence and uniqueness

The theory for saddle point structure problems is well known and can be found, for example, in [8]. To verify well-posedness, existence and unicity of the solution to such a problem, it is sufficient for certain *inf-sup* and *ell-ker* conditions to be satisfied.

To make our notation closer to the one used in [8], we introduce the following Hilbert space, with its norm:

$$\begin{aligned} \mathbb{V} &:= V \times W, \\ \|(u, w)\|_{\mathbb{V}}^2 &:= \|u\|_V^2 + \|w\|_W^2. \end{aligned}$$

We indicate with $\mathbf{u} := (u, w), \mathbf{v} := (v, y)$ the elements of \mathbb{V} , and define the following bilinear forms:

$$\begin{aligned} \mathbb{F}: \mathbb{V} \times \mathbb{V} &\longrightarrow \mathbb{R} \\ (\mathbf{u}, \mathbf{v}) &\longmapsto \langle \mathcal{K}_\Omega u, v \rangle + \langle \mathcal{K}_f w, y \rangle = (\mathbb{C}_\Omega \nabla u, \nabla v)_\Omega + (\delta \mathbb{C}_f \nabla w, \nabla y)_{\Omega_f}, \\ \mathbb{E}: \mathbb{V} \times Q &\longrightarrow \mathbb{R} \\ (\mathbf{u}, q) &\longmapsto \langle \mathcal{B} u, q \rangle - \langle \mathcal{M} w, q \rangle = \langle q, v|_{\Omega_f} - w \rangle. \end{aligned}$$

Summing the first two equations of Problem 3 and using the newly defined space we can restate the problem as: find $\mathbf{u} \in \mathbb{V}, \lambda \in Q$ such that

$$\begin{aligned} \mathbb{F}(\mathbf{u}, \mathbf{v}) + \mathbb{E}(\mathbf{v}, \lambda) &= (b, v)_\Omega & \forall \mathbf{v} := (v, y) \in \mathbb{V}, \\ \mathbb{E}(\mathbf{u}, q) &= 0 & \forall q \in Q. \end{aligned} \quad (19)$$

Following [8], to state the *inf* – *sup* conditions we introduce the kernel

$$\ker \mathbb{E} := \left\{ \mathbf{v} := (v, w) \in \mathbb{V} : \langle q, v|_{\Omega_f} - w \rangle = 0 \ \forall q \in Q \right\}.$$

Since we can identify $L^2(\Omega_f)$ with its dual, and $L^2(\Omega_f) \subset W'$, we have that for every $q \in Q$,

$$\langle q, v|_{\Omega_f} - w \rangle = 0 \Rightarrow (q, v|_{\Omega_f} - w)_{\Omega_f} = 0, \quad (20)$$

thus:

$$v|_{\Omega_f} = w \text{ a.e.}$$

There are two well-known conditions which are sufficient to prove that the problem is well-posed, and there exists a unique solution: there exist two positive constants $\alpha_1 > 0, \alpha_2 > 0$ such that

$$\inf_{q \in Q} \sup_{\mathbf{v} \in \mathbb{V}} \frac{\mathbb{E}(\mathbf{u}, q)}{\|\mathbf{u}\|_{\mathbb{V}} \|q\|_Q} \geq \alpha_1 \quad (21)$$

$$\inf_{\mathbf{u} \in \ker \mathbb{E}} \sup_{\mathbf{v} \in \ker \mathbb{E}} \frac{\mathbb{F}(\mathbf{u}, \mathbf{v})}{\|\mathbf{u}\|_{\mathbb{V}} \|\mathbf{v}\|_{\mathbb{V}}} \geq \alpha_2. \quad (22)$$

These two conditions can be proved using the following Propositions:

Proposition 2.1. *There exists a constant $\alpha_1 > 0$ such that:*

$$\inf_{q \in Q} \sup_{(v, w) \in \mathbb{V}} \frac{\langle q, v|_{\Omega_f} - w \rangle}{\|(v, w)\|_{\mathbb{V}} \|q\|_Q} \geq \alpha_1.$$

Moreover $\alpha_1 = 1$.

The proof for this proposition, and its discrete version, are variations on the one found in [10].

Proof. The non slip condition is given by the duality pairing between $Q = W'$ and W ; by definition of the norm in the dual space Q :

$$\begin{aligned} \|q\|_Q &= \sup_{w \in W} \frac{\langle q, w \rangle}{\|w\|_Q} \\ &\leq \sup_{v \in V, w \in W} \frac{\langle q, v|_{\Omega_f} - w \rangle}{(\|w\|_Q^2 + \|v\|_V^2)^{\frac{1}{2}}}, \end{aligned}$$

where the last inequality can be proven fixing $v = 0$. The final statement is found dividing by $\|q\|_Q$ and taking the $\inf_{q \in Q}$. \square

Notice that $\alpha_1 = 1$, and does not depend on the two domains or on the two spaces. Proposition 2.1 proves Inequality 21. To prove Inequality 22 additional hypotheses are needed:

Proposition 2.2. *Assume \mathbb{C}_Ω and \mathbb{C}_f to be strongly elliptical, with constants c_Ω and c_f respectively such that $c_f > c_\Omega > 0$; there exists a constant $\alpha_2 > 0$ such that:*

$$\inf_{(u,w) \in \ker \mathbb{E}} \sup_{(v,y) \in \ker \mathbb{E}} \frac{(\mathbb{C}_\Omega \nabla u, \nabla v)_\Omega + (\delta \mathbb{C}_f \nabla w, \nabla y)_{\Omega_f}}{\|(v,y)\|_{\mathbb{V}} \|(u,w)\|_{\mathbb{V}}} \geq \alpha_2.$$

Proof. An immediate consequence of the hypotheses is that $\delta \mathbb{C}_f$ is elliptic of constant $c_f - c_\Omega$. Following the proof for a similar statement found in [4, 12], given an element $(v,y) \in \ker(\mathbb{E})$, the fact that $v|_{\Omega_a} = y$ allows to use the Poincaré inequality on v to control the norm of y ; for every $(u,w) \in \ker(\mathbb{E})$:

$$\begin{aligned} & \sup_{(v,y) \in \ker(\mathbb{E})} \frac{(\mathbb{C}_\Omega \nabla u, \nabla v)_\Omega + (\delta \mathbb{C}_f \nabla w, \nabla y)_{\Omega_f}}{\|(v,y)\|_{\mathbb{V}}} \\ & \geq \frac{c_\Omega (\nabla u, \nabla u)_\Omega + (c_f - c_\Omega) (\nabla w, \nabla w)_{\Omega_f}}{\|(u,w)\|_{\mathbb{V}}} \\ & \geq \frac{c_p \min(c_\Omega, c_f - c_\Omega)}{2} \frac{(u,u)_{H^1(\Omega)} + (w,w)_{H^1(\Omega_f)}}{\|(u,w)\|_{\mathbb{V}}} \\ & \geq \alpha_2 \|(u,w)\|_{\mathbb{V}}, \end{aligned}$$

where we used the Poincaré inequality with its positive constant c_p on $u \in V$, with $\alpha_2 := \frac{c_p \min(c_\Omega, c_f - c_\Omega)}{2}$, and we used the scalar product of $H^1(\Omega)$:

$$(u,u)_{H^1(\Omega)} := (u,v)_\Omega + (\nabla u, \nabla v)_\Omega,$$

and the analogous one for $H^1(\Omega_f)$. The final statement is obtained dividing by $\|(u,w)\|_{\mathbb{V}}$ and considering the $\inf_{(u,w) \in \ker \mathbb{E}}$. \square

Remark. *This paper does not intend to focus on the choice of elastic tensors. Strong ellipticity is a common property among them, and holds in the case of linearly elastic materials (see e.g. [41]): let $u \in V$, $w \in W$*

$$\mathbb{C}_\Omega \nabla u := 2\mu_\Omega E u + \lambda_\Omega (\text{tr} \nabla u) I = 2\mu_\Omega E u + \lambda_\Omega (\text{div} u) I \quad (23)$$

$$\mathbb{C}_f \nabla w := 2\mu_f E w + \lambda_f (\text{tr} \nabla w) I = 2\mu_f E w + \lambda_f (\text{div} w) I \quad (24)$$

$$\begin{aligned} \delta \mathbb{C}_f \nabla w &:= 2(\mu_f - \mu_\Omega) E w + (\lambda_f - \lambda_\Omega) (\text{tr} \nabla w) I \\ &= 2\mu_\delta E w + \lambda_\delta (\text{div} w) I, \end{aligned} \quad (25)$$

where $\mu_\delta := \mu_f - \mu_\Omega$ and $\lambda_\delta := \lambda_f - \lambda_\Omega$. These are the elastic tensors we shall use in Section 4, for our numerical tests.

Proposition 2.2 implies Inequality 22, and we conclude that Problem 3 is well-posed, and has a unique solution.

2.3. Finite element discretization

The formulation of Problem 3 makes it possible to consider independent, separate triangulations for its numerical solution. Consider the family $\mathcal{T}_h(\Omega)$ of regular meshes in Ω , and a family $\mathcal{T}_h(\Omega_f)$ of regular meshes in Ω_f , where we denote by h the maximum diameter of the elements of the two triangulations. We assume that no geometrical error is committed when meshing, i.e., $\Omega = \bigcup_{T_h \in \mathcal{T}_h(\Omega)} T_h$, and $\Omega_f = \bigcup_{S_h \in \mathcal{T}_h(\Omega_f)} S_h$. We consider two independent finite element spaces $V_h \subset V$, and $W_h \subset W$.

For every element of W , the duality pairing between Q and W can be represented using the L^2 scalar product in Ω_a :

$$\langle q, w \rangle = (q, w)_{\Omega_a}.$$

Thus we discretize the duality pairing as the L^2 product, and consider $Q_h = W_h$. To handle the restriction of functions from V_h to W_h , we first introduce the L^2 projection:

$$P_W: W \rightarrow W_h \subset L^2(\Omega_f),$$

which is continuous: for every $u \in L^2(\Omega_f)$

$$\|P_W u\|_{L^2(\Omega_f)} \leq \|u\|_{L^2(\Omega_f)}.$$

This condition is too weak for our problem, which involves ∇w . We make the further assumption that the restriction $P_W|_W \neq 0$, and we assume it is H^1 -stable, i.e., there exists a positive constant c , such that for all $w \in W$:

$$\|\nabla P_W|_W w\|_{\Omega_f} \leq c \|\nabla w\|_{\Omega_f}. \quad (26)$$

With a slight abuse of notation we use P_W instead of $P_W|_W$. We assume that the H^1 -stability property holds uniformly on $\mathcal{T}_h(\Omega)$ and $\mathcal{T}_h(\Omega_f)$, provided that the mesh size h is comparable on the two domains.

To discretize Problem 3, we reformulate the weak non-slip condition of Equation 11: for every $v_h \in V_h, w_h \in W_h, q_h \in Q_h$:

$$\begin{aligned} (q_h, v_h|_{\Omega_f} - w_h)_{\Omega_f} &= (q_h, v_h|_{\Omega_f})_{\Omega_f} - (q_h, w_h)_{\Omega_f} \\ &= (q_h, P_W v_h)_{\Omega_f} - (q_h, w_h)_{\Omega_f} = (q_h, P_W v_h - w_h)_{\Omega_f}. \end{aligned}$$

Problem 4 (Discrete Weak Formulation). *Given $b \in L^2(\Omega)^d$, find $u_h \in V_h, w_h \in W_h, \lambda_h \in Q_h$ such that:*

$$(\mathbb{C}_\Omega \nabla u_h, \nabla v_h)_\Omega + (\lambda_h, P_W v_h)_{\Omega_f} = (b, v_h)_\Omega \quad \forall v_h \in V_h, \quad (27)$$

$$(\delta \mathbb{C}_f \nabla w_h, \nabla y_h)_{\Omega_f} - (\lambda_h, y_h)_{\Omega_f} = 0 \quad \forall y_h \in W_h, \quad (28)$$

$$(q_h, P_W u_h - w_h)_{\Omega_f} = 0 \quad \forall q_h \in Q_h. \quad (29)$$

As in the continuous case, we study the *inf* – *sup* conditions after defining the following space:

$$\mathbb{V}_h := V_h \times W_h,$$

equipped with the norm $\|\cdot\|_{\mathbb{V}}$, and the operators:

$$\begin{aligned}\mathbb{F}_h &: \mathbb{V}_h \times \mathbb{V}_h \longrightarrow \mathbb{R} \\ (\mathbf{u}_h, \mathbf{v}_h) &\longmapsto (\mathbb{C}_\Omega \nabla \mathbf{u}_h, \nabla \mathbf{v}_h)_\Omega + (\delta \mathbb{C}_f \nabla w_h, \nabla y_h)_{\Omega_f}, \\ \mathbb{E}_h &: \mathbb{V}_h \times Q_h \longrightarrow \mathbb{R} \\ (\mathbf{u}_h, q_h) &\longmapsto (q_h, P_W v_h - w_h)_{\Omega_f}.\end{aligned}$$

Equation 19 can now be discretized: find $\mathbf{u}_h \in \mathbb{V}_h, \lambda_h \in Q_h$ such that

$$\begin{aligned}\mathbb{F}_h(\mathbf{u}_h, \mathbf{v}_h) + \mathbb{E}_h(\mathbf{v}_h, \lambda_h) &= (b, v_h)_\Omega, & \forall \mathbf{v}_h := (v_h, y_h) \in \mathbb{V}_h \\ \mathbb{E}_h(\mathbf{u}_h, q_h) &= 0 & \forall q_h \in Q_h.\end{aligned}$$

Following Subsection 2.2, Problem 4 is well-posed, and there exists a unique solution if there exist two positive constants $\alpha_3 > 0, \alpha_4 > 0$ such that

$$\begin{aligned}\inf_{q_h \in Q_h} \sup_{\mathbf{v}_h \in \mathbb{V}_h} \frac{\mathbb{E}(\mathbf{u}_h, q_h)}{\|\mathbf{u}_h\|_{\mathbb{V}} \|q_h\|_{\Omega_f}} &\geq \alpha_3 \\ \inf_{\mathbf{u}_h \in \ker \mathbb{E}_h} \sup_{\mathbf{v}_h \in \ker \mathbb{E}_h} \frac{\mathbb{F}(\mathbf{u}_h, \mathbf{v}_h)}{\|\mathbf{u}\|_{\mathbb{V}_h} \|\mathbf{v}_h\|_{\mathbb{V}_h}} &\geq \alpha_4.\end{aligned}$$

These conditions can be proved modifying Propositions 2.1 and 2.2:

Proposition 2.3. *There exists a constant $\alpha_3 > 0$, independent of h , such that:*

$$\inf_{q_h \in Q_h} \sup_{(v_h, w_h) \in \mathbb{V}_h} \frac{(q_h, P_W v_h - w_h)_{\Omega_f}}{\|(v_h, w_h)\|_{\mathbb{V}} \|q_h\|_{\Omega_f}} \geq \alpha_3.$$

Proof. The proof is similar to the one of Proposition 2.1. For every $q_h \in Q_h$, by definition of the Q norm, there exists $\hat{w} \in W$ such that:

$$\|q_h\|_Q = \sup_{w_h \in W_h} \frac{(q_h, w_h)_{\Omega_f}}{\|w_h\|_Q} = \frac{(q_h, \hat{w})_{\Omega_f}}{\|\hat{w}\|_Q} = \frac{(q_h, P_W \hat{w})_{\Omega_f}}{\|\hat{w}\|_Q}. \quad (30)$$

Using well-known properties of P_W , and the H^1 stability, we can prove there exists a c such that:

$$\|P_W \hat{w}\|_Q \leq C \|\hat{w}\|_Q.$$

Inserting this in Equation 30:

$$\begin{aligned}\|q_h\|_Q &\leq \frac{(q_h, P_W \hat{w})_{\Omega_f}}{\|\hat{w}\|_Q} \leq C \frac{(q_h, P_W \hat{w})_{\Omega_f}}{\|P_W \hat{w}\|_Q} \\ &\leq C \sup_{w_h \in W_h} \frac{(q_h, w_h)_{\Omega_f}}{\|w_h\|_Q} \leq C \sup_{v_h \in V_h, w_h \in W_h} \frac{(q_h, v_h|_{\Omega_a} - w_h)_{\Omega_f}}{(\|w_h\|_Q^2 + \|v_h\|_V^2)^{\frac{1}{2}}},\end{aligned}$$

and we conclude as in Proposition 2.1. \square

To study the *ell - ker* condition on \mathbb{F}_h we define:

$$\begin{aligned}\ker(\mathbb{E}_h) &:= \{\mathbf{v}_h := (v_h, w_h) \in \mathbb{V}_h : (q_h, P_W v_h - w_h)_{\Omega_f} = 0 \quad \forall q_h \in Q_h\} \\ &= \{\mathbf{v}_h := (v_h, w_h) \in \mathbb{V}_h : (q_h, P_W v_h)_{\Omega_f} = (q_h, w_h)_{\Omega_f} \quad \forall q_h \in Q_h\}.\end{aligned}$$

Proposition 2.4. *Assume \mathbb{C}_Ω and \mathbb{C}_f to be strongly elliptical with constants c_Ω and c_f respectively such that $c_f > c_\Omega > 0$; there exists a constant $\alpha_4 > 0$, independent of h , such that:*

$$\inf_{(u_h, w_h) \in \ker(\mathbb{E})_h} \sup_{(v_h, y_h) \in \ker(\mathbb{E})_h} \frac{(\mathbb{C}_\Omega \nabla v_h, \nabla u_h)_\Omega + (\delta \mathbb{C}_f \nabla y_h, \nabla w_h)_{\Omega_f}}{\|(v_h, y_h)\|_{\mathbb{V}} \|(u_h, w_h)\|_{\mathbb{V}}} \geq \alpha_4.$$

Proof. *Mutatis mutandis*, the proof follows the one of Proposition 2.2. \square

Error estimate. Proposition 2.1 and 2.2 allow us to apply the theory from Chapter 5 of [8], obtaining the following error estimate:

Theorem 2.1. *Consider \mathbb{C}_Ω and \mathbb{C}_f , elastic stress tensors satisfying the hypothesis of Proposition 2.2, the domains Ω and Ω_f with the regularity required in Section 2, and $b \in L^2(\Omega)^d$. Then the following error estimate holds for (u, w, λ) , solution to Problem 3, and (u_h, w_h, λ_h) , solution of Problem 4:*

$$\|u - u_h\|_V + \|w - w_h\|_W + \|\lambda - \lambda_h\|_Q \leq C_e \left(\inf_{v_h \in V_h} \|u - v_h\|_V + \inf_{y_h \in W_h} \|w - y_h\|_W + \inf_{q_h \in Q_h} \|\lambda - q_h\|_Q \right), \quad (31)$$

where $C_e > 0$, and depends on $\alpha_3, \alpha_4, c_\Omega, c_f$ and the norm of the operators \mathcal{K}_Ω and \mathcal{K}_f .

We remark how the constant C_e is affected by the coupling between the two meshes; as intuition suggests, the quality of the solution does not depend only on the ability of V and W to individually describe it, but also on the coupling between them.

Non-matching meshes. One of the basic assumptions made in the continuous case is that, for every element $v \in V$, we have that $v|_{\Omega_a} \in W$; similarly every element $w \in W$ can be extended to an element of V .

With an independent discretization of the two meshes the inclusion $W_h \subset V_h$ can not be guaranteed, leading to the use of the projection $P_W: V_h \rightarrow W_h$, which we require to be H^1 -stable, i.e., that Equation 26 holds.

Since for every $\mathbf{v}_h = (v_h, w_h) \in \ker(\mathbb{E}_h) \Rightarrow P_W(v_h) = w_h \Rightarrow w_h \in P_W(V_h)$; if the set $P_W(V_h)$ is small, the *inf* – *sup* constant can be negatively affected; the extreme case being $P_W = 0$, which results in $\ker(\mathbb{E}_h) = \{(0, 0)\}$, and the *inf* – *sup* condition for \mathbb{F}_h not satisfied.

Under some simple construction hypotheses it is possible to guarantee that globally constant and linear functions are included in the kernel, ensuring that $\ker(\mathbb{E}_h) \neq \{(0, 0)\}$.

3. Thin fibers

The computational cost of discretizing explicitly numerous three-dimensional fibers might render Problem 4 too computationally demanding: a possible simplification is suggested by the fiber shape, which can be approximated with a one-dimensional structure. Constructing this simplified model is a non-trivial task because the restriction (or trace) of a three-dimensional function to a one-dimensional domain is not well defined in Sobolev spaces.

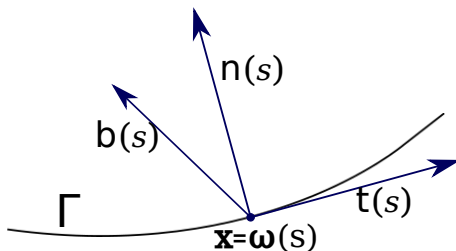


Figure 3: The Frenet trihedron.

Instead of resorting to weighted Sobolev spaces and graded meshes, as done in [15, 14], the solution we propose is to introduce additional modellistic hypotheses, that allow one to use averaging techniques instead of traces to render the problem well posed.

To simplify the exposition, we shall consider a single fiber; the same results hold with a finite collection of fibers.

3.1. Some notions of differential geometry

The description of our model requires requires some basic notions of differential geometry, which we briefly collect here; for a more detailed reference see, e.g., [33].

Consider Γ , a one-dimensional curve immersed in \mathbb{R}^3 ; let $I \subset \mathbb{R}$ be a finite interval, and $\omega: I \rightarrow \Gamma$ be the arclength parametrization of Γ .

Assuming the curve is C^3 , at each point $x \in \Gamma$, there exists an $s \in I$ such that $x = \omega(s)$; and the curve parametrization defines a base for \mathbb{R}^3 , called the Frenet trihedron:

$$\begin{aligned} t(s) &= \frac{d\omega(s)}{ds} \\ n(s) &= \frac{dt(s)}{ds} \Big/ \left\| \frac{dt(s)}{ds} \right\| \\ b(s) &= t(s) \times n(s). \end{aligned}$$

Here t is the vector tangent to the curve at x , while n and b generate the plane orthogonal to the curve at x ; for an example see Figure 3.

To describe the curve Γ it is useful to introduce the notions of *curvature*:

$$\kappa(s) := \left\| \frac{d^2\omega(s)}{ds^2} \right\|,$$

and *torsion*:

$$\tau(s) := - \left(\frac{d}{ds} b(s) \right) \cdot n(s).$$

A curve with torsion identically zero is called *planar curve*, as it can be embedded inside a plane.

To describe the evolution of curvature and torsion along the curve, we use the so-called *Frenet-Serret* formulas:

$$\begin{aligned}\frac{dt(s)}{ds} &= \kappa(s)n(s), \\ \frac{dn(s)}{ds} &= -\kappa(s)t(s) + \tau(s)b(s), \\ \frac{db(s)}{ds} &= -\tau(s)n(s).\end{aligned}\tag{32}$$

The concept of tubular neighbourhoods is one of the basic tools in differential geometry; the basic properties of a tubular neighbourhoods which we report here are often shown as examples of exercises in multidimensional real analysis and multivariable calculus books, e.g., [16].

Given a radius $a \in \mathbb{R}$, $a > 0$, and a curve Γ in \mathbb{R}^3 , we define the tubular neighbourhood of Γ of radius a , as the set of all points in \mathbb{R}^3 at distance at most a from the curve:

$$\Omega_a := \{x \in \mathbb{R}^3: \text{dist}(x, \Gamma) \leq a\}.$$

If Γ is regular enough, and has an arclength parametrization ω , then Ω_a can also be defined as:

$$\Omega_a := \{\omega(s) + n(s)\lambda_1 + b(s)\lambda_2: s \in I; \lambda_1, \lambda_2 \in \mathbb{R} \text{ s.t. } \sqrt{\lambda_1^2 + \lambda_2^2} \leq a\}.$$

We require $\partial\Omega_a$ to be non-intersecting. This hypothesis is satisfied locally if ω is either C^3 regular or a C^2 regular plane curve, and the radius is chosen such that

$$a < \max_{s \in I} \frac{1}{\kappa(s)}.$$

For a plane curve, the osculating circle has radius $\max_{s \in I} \frac{1}{\kappa(s)}$, and can be seen as the intersection of normals for infinitely closed points; because a is smaller than the radius, perpendicular disks do not intersect.

If the torsion τ is non-zero, then we can repeat the argument in space using the osculating sphere, which has radius:

$$R(s) = \sqrt{\frac{1}{\kappa(s)^2} + \frac{1}{(\kappa'(s)\tau(s))^2}},$$

after noticing that $R(s) \geq \frac{1}{\kappa(s)}$.

To describe the tubular neighbourhood, we introduce the following definition: for all $x = \omega(s) \in \Gamma$, we define $D_a(x)$ as the two-dimensional disk perpendicular to Γ , with radius a , centered at x :

$$D_a(x) := \{\omega(s) + n(s)\lambda_1 + b(s)\lambda_2: \lambda_1, \lambda_2 \in \mathbb{R}, \sqrt{\lambda_1^2 + \lambda_2^2} \leq a\}.$$

The use of Frenet-Serret coordinates is used in physics to study wave propagation, optics and particle trajectories [36].

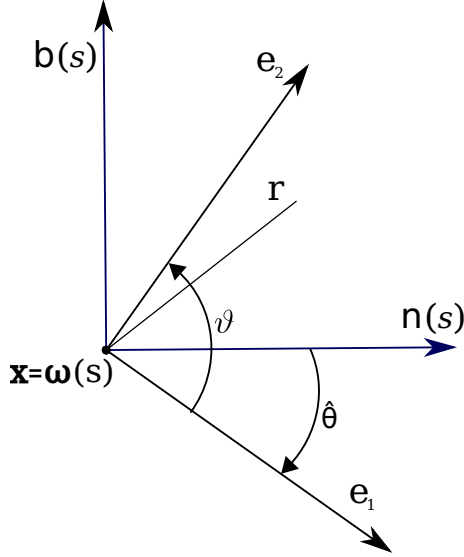


Figure 4: Frenet-Serret and the rotated coordinate systems.

To simplify our computations we shall rotate the orthogonal vectors, as proposed by Tang [54], and then transform the plane $\langle n, b \rangle$ using polar coordinates, as done in [52].

Recall that each point x of the tubular neighbourhood Ω_a can be written as

$$x = \omega(s) + x_0 n(s) + y_0 b(s),$$

with $x_0, y_0 \in [-a, a]$, where x_0 and y_0 are the distances from x to the centerline Γ , along the normal and binormal directions. Using the Frenet-Serret formulas 32, we can compute the metric tensor:

$$dx \cdot dx = dx_0^2 + dy_0^2 + [(1 - \kappa x_0)^2 + (x_0^2 + y_0^2)\tau^2]ds^2 + 2\tau(x_0 dy_0 - y_0 dx_0)ds.$$

The metric is non-orthogonal because of the mixed term $2\tau(x_0 dy_0 - y_0 dx_0)ds$.

To obtain an orthogonal metric, define θ as an angle solving the following differential equation:

$$\begin{aligned} \frac{d\theta(s)}{ds} &= \tau(s), \\ \theta(0) &= \hat{\theta}. \end{aligned}$$

where the initial value $\hat{\theta}$ can be fixed arbitrarily. Define the rotated vectors:

$$e_1(s) = \cos(\theta(s))n(s) - \sin(\theta(s))b(s) \quad (33)$$

$$e_2(s) = \sin(\theta(s))n(s) + \cos(\theta(s))b(s), \quad (34)$$

each point $x \in \Omega_a$ can be written in the new system of reference as:

$$x = \omega(s) + x_1 e_1 + y_1 e_2.$$

The metric of the the coordinates (t, e_1, e_2) is orthogonal:

$$dx \cdot dx = dx_1^2 + dy_1^2 + [1 - \kappa(x_1 \cos(\theta) + y_1 \sin(\theta))]^2 ds^2.$$

We assume fibers to be cylindrical in their reference configuration; a natural development for our model is for fibers to be axisymmetric. This suggests the use of a coordinate system where the orthogonal plane to a point x of the curve, is described through polar coordinates.

Consider the coordinate system (r, ϑ, s) , where (r, ϑ) are defined so that:

$$x_1 = r \cos(\vartheta) \tag{35}$$

$$y_1 = r \sin(\vartheta). \tag{36}$$

This coordinate system is shown in Figure 4; the metric for the coordinate system (r, ϑ, s) is:

$$dx \cdot dx = dr^2 + r^2 d\vartheta^2 + (1 - \kappa r \cos(\vartheta - \hat{\theta}))^2 ds^2.$$

This allows to write the gradient in the coordinates (r, ϑ, s) :

$$\nabla \cdot := \frac{d \cdot}{dr} e_1 + \frac{1}{r} \frac{d \cdot}{d\vartheta} e_2 + \frac{1}{1 - \kappa(s)r \cos(\vartheta - \hat{\theta})} \frac{d \cdot}{ds} t.$$

3.2. Introducing the setting

As in the previous section, we let Γ be a one-dimensional connected domain, embedded in Ω , let $\omega: [0, L] \rightarrow \Gamma$ be its arclength parametrization of Γ . We assume the Frenet trihedron $(t(s), n(s), b(s))$ to be well defined for every $s \in [0, L]$, at every point $\omega(s) \in \Gamma$, and the function $s \mapsto (t(s), n(s), b(s))$ to be continuous.

We fix a constant radius $a \in \mathbb{R}$, $a > 0$ for the physical fiber Ω_a , which is described by the tubular neighbourhood of Γ or radius a ; we assume $\Omega_a \subset \Omega$.

We now modify the definitions of Section 2, for the boundaries of $\partial\Omega_a$:

$$\begin{aligned} B_i &:= \partial\Omega_a \setminus \partial\Omega, \\ B_e &:= \partial\Omega \cap \partial\Omega_a, \\ V &:= (H_{0, \partial\Omega}^1(\Omega))^d, \\ W &:= (H_{0, B_e}^1(\Omega_2))^d, \end{aligned}$$

with $d = 3$.

As a reference model, we consider small deformations of an FRM in which fibers are stiff compared to the underlying matrix. For this model, the fiber radius can be considered to be approximately constant.

Curved fiber. In this section we call Γ be a one-dimensional straight line, immersed in \mathbb{R}^3 of finite length, and call Ω_a its tubular neighbourhood of radius a , which is a straight cylinder. To represent a generic a one-dimensional connected domain we use the symbol $\tilde{\Gamma}$, and assume its tubular neighborhood can be obtained through the restriction of the diffeomorphism

$$\Phi: \Omega \rightarrow \tilde{\Omega}, \quad (37)$$

satisfying the following hypotheses:

- It transforms the cylinder into the tubular neighbourhood of the curve $\tilde{\Gamma}$ with constant radius a : $\tilde{\Omega}_a = \Phi(\Omega_a)$
- It transforms the cylinder center line: $\tilde{\Gamma} = \Phi(\Gamma)$
- It transforms orthogonal disks to Γ into orthogonal disks to $\tilde{\Gamma}$: for every $x \in \Gamma$, $D_{a,\tilde{\Gamma}}(\Phi(x)) = \Phi(D_{a,\Gamma}(x)) \Rightarrow \Phi^{-1}\left(D_{a,\tilde{\Gamma}}(\Phi(x))\right) = D_{a,\Gamma}(x)$,

where we added the subscript to identify the disk as orthogonal to $\tilde{\Gamma}$ and Γ respectively; $D_{a,\tilde{\Gamma}}(\Phi(x)) \subset \tilde{\Omega}_a$, and $D_{a,\Gamma}(\Phi(x)) \subset \Omega_a$.

Numerous transformations satisfy these properties, e.g., rotations and stretches, but also transformations modifying the curvature.

To simplify the notation we shall avoid making the explicit distinction between Γ , $\tilde{\Gamma}$ etc. in this manuscript, except for this paragraph and the next subsection, preferring then the symbol without tilde.

3.3. Regularity of the average

In this subsection we prove that, by considering a certain average for our functions, we obtain a sufficiently regular “restriction” operator which we can use for our fictitious domain approach.

To avoid confusion, in this subsection we shall avoid the symbols V, W , writing explicitly the spaces as $H^1(\Omega)$, $H^1(\tilde{\Omega}_a)$, and so on.

In this Section, domains without tilde, such as Γ , refer to the case of cylinder aligned with the first axis; domains with tilde, such as $\tilde{\Gamma}$, are used for other domains.

Let $w \in H^1(\tilde{\Gamma})$ (or $w \in H^1(\Gamma)$), the surface gradient along the curve is defined as:

$$\nabla_{\tilde{\Gamma}} w := t \otimes t \nabla \bar{w}, \quad (38)$$

where \bar{w} is a tubular extension of w on a neighbourhood of $\tilde{\Gamma}$ (or Γ), and we are using the unitary tangent vector to the curve $\tilde{\Gamma}$ from the Frenet trihedron $(t(x), n(x), b(x))$.

We now want to prove that for every $u \in H^1(\tilde{\Omega})$, its average on $\tilde{\Gamma}$ is also on $H^1(\tilde{\Gamma})$, i.e., $\bar{u} \in H^1(\tilde{\Gamma})$, where \bar{u} is defined for a.e. $x \in \Gamma$ as:

$$\bar{u}(x) := \frac{1}{|D_a(0)|} \int_{D_a(x)} u(y) dD_y. \quad (39)$$

We first use cylinders aligned with the first axis, using the axis-aligned coordinates (x_1, x_2, x_3) , and consider only the case $\Omega_a \Subset \Omega$ with functions defined on $H^1(\Omega_a) :=$

$H^1(\Omega)|_{\Omega_a}$ (the extension to $H_0^1(\Omega)$ is trivial). The results hold also in the case $H_{B_e}^1(\Omega_a)$, which can be proven with few changes.

The following lemma is used to prove that, if u is C^∞ , then $\bar{u} \in H^1(\Gamma)$; later we shall extend the result to H^1 using density.

Lemma 3.1. *Let $u \in C^\infty(\bar{\Omega}_a)$, then the following inequalities hold:*

$$\|\bar{u}\|_\Gamma \leq \frac{1}{\sqrt{\pi a}} \|u\|_{\Omega_a} \quad (40)$$

$$\|\nabla_\Gamma \bar{u}\|_\Gamma \leq \frac{1}{\sqrt{\pi a^2}} \|\nabla u\|_{\Omega_a} \quad (41)$$

Proof. Since we use C^∞ , we can consider their restrictions: the first coordinate, x_1 , shall be used for the cylinder axis, while x_2 and x_3 are normal to the axis. The first inequality can be proven directly, using either Jensen's or Hölder inequality:

$$\begin{aligned} \|\bar{u}\|_\Gamma^2 &= \frac{1}{(\pi a^2)^2} \int_\Gamma \left(\int_{D_a(x_1)} u(x_1, x_2, x_3) dx_2 dx_3 \right)^2 dx_1 \\ &\leq \frac{1}{\pi a^2} \int_\Gamma \int_{D_a(x_1)} u(x_1, x_2, x_3)^2 dx_2 dx_3 dx_1 = \frac{1}{\pi a^2} \|u\|_{\Omega_a}^2 \end{aligned}$$

The second inequality can be proven in a similar fashion, after recognizing that, for every $x \in \Gamma$, the integral domain $D_a(x_1)$, used to compute $\bar{u}(x)$ does not depend on the variable x_1 , and that $|\nabla_\Gamma \bar{u}(x)|^2 = |\partial_{x_1} \bar{u}(x)|^2$.

Define $D := \{x_2, x_3 \text{ s.t. } x_2^2 + x_3^2 \leq a^2\}$, then:

$$\begin{aligned} \|\nabla_\Gamma \bar{u}\|_\Gamma^2 &= \frac{1}{(\pi a^2)^2} \int_\Gamma \left(\partial_{x_1} \int_{D_a(x_1)} u(x_1, x_2, x_3) dx_2 dx_3 \right)^2 dx_1 \\ &= \frac{1}{(\pi a^2)^2} \int_\Gamma \left(\partial_{x_1} \int_{(x_2, x_3) \in D} u(x_1, x_2, x_3) dx_2 dx_3 \right)^2 dx_1 \\ &= \frac{1}{(\pi a^2)^2} \int_\Gamma \left(\int_{(x_2, x_3) \in D} \partial_{x_1} u(x_1, x_2, x_3) dx_2 dx_3 \right)^2 dx_1 \\ &\leq \frac{1}{\pi a^2} \int_\Gamma \int_{(x_2, x_3) \in D} \partial_{x_1} u(x_1, x_2, x_3)^2 dx_2 dx_3 dx_1 \leq \frac{1}{\pi a^2} \|\nabla u\|_{\Omega_a}^2 \end{aligned}$$

□

Proposition 3.1. *Consider a straight cylinder Ω_a ; then*

$$u \in H^1(\Omega_a) \Rightarrow \bar{u} \in H^1(\Gamma).$$

Proof. We begin considering $u \in C^\infty(\bar{\Omega}_a)$. Using Lemma 3.1 we obtain:

$$\|\bar{u}\|_{H^1(\Gamma)} \leq \frac{1}{\sqrt{\pi a}} \|u\|_{H^1(\Omega_a)},$$

therefore $\bar{u} \in H^1(\Gamma)$.

Consider now a generic $u \in H^1(\Gamma)$, then there exists a sequence of functions $(u_n)_{n \in \mathbb{N}} \subset C^\infty(\bar{\Omega}_a)$ such that $u_n \xrightarrow{H^1} u$, and we conclude with a density argument. \square

We now want to extend Proposition 3.1 to the case of a tubular neighborhood obtained through a diffeomorphism Φ satisfying the hypotheses at the beginning of this section.

To generalize our result on straight cylinders we use the following Lemma:

Lemma 3.2. *Given Φ diffeomorphism with the above hypotheses, for every $u \in H^1(\tilde{\Omega}_a)$:*

$$\|u \circ \Phi\|_{H^1(\Omega_a)} \leq C_J^{1/2} C_\Phi \|u\|_{H^1(\tilde{\Omega}_a)} \quad (42)$$

$$\|\bar{u}\|_{H^1(\tilde{\Gamma})} \leq (C_J C_\Phi)^{3/2} \|\overline{u \circ \Phi}\|_{H^1(\Gamma)}, \quad (43)$$

where we defined the following positive constants:

$$C_J := \sup_{z \in \tilde{\Omega}_a} |J\Phi^{-1}(z)| \quad C_\Phi := \sup_{z \in \tilde{\Omega}_a} |\nabla\Phi(z)|.$$

Proof. The proof for the two inequality is, essentially, a change of variables using Φ^{-1} . For the first inequality, we begin with the L^2 part of the norm:

$$\|u \circ \Phi\|_{\Omega_a}^2 = \int_{\Omega_a} (u \circ \Phi)^2 d\Omega = \int_{\tilde{\Omega}_a} u^2 |J\Phi^{-1}| d\tilde{\Omega} \leq C_J \|u\|_{\tilde{\Omega}_a}^2.$$

Similarly, for $\|\nabla(u \circ \Phi)\|_{\Omega_a}^2$:

$$\begin{aligned} \|\nabla(u \circ \Phi)\|_{\Omega_a}^2 &= \int_{\Omega_a} (\nabla(u \circ \Phi)(z))^2 d\Omega_z \\ &= \int_{\Omega_a} (\nabla\Phi(z)^T \nabla u(\Phi(z)))^2 d\Omega_z \leq C_\Phi^2 \int_{\Omega_a} (\nabla u(\Phi(z)))^2 d\Omega_z \\ &= \int_{\tilde{\Omega}_a} (\nabla u(\tilde{z}))^2 |J\Phi^{-1}| d\tilde{\Omega} \leq C_J C_\Phi^2 \|u\|_{\tilde{\Omega}_a}^2. \end{aligned}$$

To prove the second inequality we split the change of variables, considering the restrictions of Φ first to the disks, and then to the centerline of the tubular neighbourhood. The symbols we use for these restrictions are, respectively, Φ_D and Φ_Γ . With a slight abuse of notation we avoid to describe the exact disk used for the restriction.

$$\begin{aligned} \|\bar{u}\|_{\tilde{\Gamma}}^2 &= \int_{\tilde{\Gamma}} \bar{u}(\tilde{x})^2 d\tilde{x} = \int_{\tilde{\Gamma}} \left(\frac{1}{\pi a^2} \int_{D_{a,\tilde{\Gamma}}(\tilde{x})} u(\tilde{y}) dD\tilde{y} \right)^2 dx \\ &= \int_{\tilde{\Gamma}} \left(\frac{1}{\pi a^2} \int_{\Phi^{-1}(D_{a,\tilde{\Gamma}}(\tilde{x}))} u(\Phi(y)) |J\Phi_D| dDy \right)^2 d\tilde{x} \\ &= \int_{\Gamma} \left(\frac{1}{\pi a^2} \int_{\Phi^{-1}(D_{a,\tilde{\Gamma}}(\Phi(x)))} u(\Phi(y)) |J\Phi_D| dDy \right)^2 |J\Phi_\Gamma| dx \\ &\leq C_J^3 \int_{\Gamma} \left(\frac{1}{\pi a^2} \int_{D_{a,\Gamma}(x)} u(\Phi(y)) dDy \right)^2 dx = C_J^3 \|\overline{u \circ \Phi}\|_{\tilde{\Gamma}}^2, \end{aligned}$$

where we used the fact that, by hypothesis, $\Phi^{-1}\left(D_{a,\tilde{\Gamma}}(\Phi(x))\right) = u(\Phi(y))$. To conclude we apply the same procedure to the gradient norm. \square

Proposition 3.2. *Consider a cylinder $\tilde{\Omega}_a$, and Φ with properties above; then:*

$$u \in H^1(\tilde{\Omega}_a) \Rightarrow \bar{u} \in H^1(\tilde{\Gamma}).$$

Proof. Notice that $u \circ \Phi$ is defined on a straight cylinder.

Combining Lemma 3.2 and Lemma 3.1:

$$\begin{aligned} \|\bar{u}\|_{H^1(\tilde{\Gamma})} &\leq (C_J C_\Phi)^{3/2} \|\overline{u \circ \Phi}\|_{H^1(\Gamma)} \leq \frac{(C_J C_\Phi)^{3/2}}{\sqrt{\pi a}} \|u \circ \Phi\|_{H^1(\Omega_a)} \\ &\leq \frac{C_J^2 C_\Phi^{5/2}}{\sqrt{\pi a}} \|u \circ \Phi\|_{H^1(\tilde{\Omega}_a)}, \end{aligned}$$

which concludes the proof. \square

3.4. Gradient equality

In the case of straight cylinders, after aligning the axis, it is possible to prove the following equation:

$$\frac{1}{2}(\delta\mathbb{C}_f \nabla Ew, \nabla Ew)_{\Omega_a} = \frac{c_\Gamma}{2}(\delta\mathbb{C}_f \nabla_\Gamma w, \nabla_\Gamma w)_\Gamma, \quad (44)$$

where $c_\Gamma := \pi a^2$.

This is not true in general but, as we shall prove, it is possible to define a function g defined on Γ , which allows to reduce the integral to a one-dimensional one, by describing the geometry of the tubular neighbourhood.

Proposition 3.3. *For a general tubular neighborhood Ω_a of a curve Γ , for which curvature κ and torsion τ are defined a.e., there exists a function g defined on Γ satisfying:*

$$\frac{1}{2}(\delta\mathbb{C}_f \nabla Ew, \nabla Ew)_{\Omega_a} = \frac{c_\Gamma}{2}(g \delta\mathbb{C}_f \nabla_\Gamma w, \nabla_\Gamma w)_\Gamma. \quad (45)$$

Proof. Let $\omega: I \rightarrow \Gamma$ be the arclength parametrization of Γ ; the proof is based on the idea of computing $(\delta\mathbb{C}_f \nabla Ew, \nabla Ew)_{\Omega_a}$ on the reference based on the Frenet trihedron.

In this reference, consider an element $w \in H^1(\Gamma)$, and its extension as constant on each orthogonal disk Ew :

$$\begin{aligned} \nabla Ew &:= \frac{dEw}{dr} \mathbf{e}_r + \frac{1}{r} \frac{dEw}{d\theta} \mathbf{e}_\theta + \frac{1}{1 - \kappa(s)r \cos(\theta - \hat{\theta})} \frac{dEw}{ds} \mathbf{e}_s \\ &= \frac{1}{1 - \kappa(s)r \cos(\theta - \hat{\theta})} \frac{dEw}{ds} \mathbf{e}_s. \end{aligned}$$

For every vector component of the gradient (for simplicity we avoid adding a specific index):

$$\begin{aligned}
(\delta\mathbb{C}_f \nabla Ew, \nabla Ew)_{\Omega_a} &= \int_{\Omega_a} \delta\mathbb{C}_f \nabla Ew \nabla Ew d\Omega \\
&= \int_{\Gamma} \left(\int_{D_a(s)} \delta\mathbb{C}_f \nabla_{\Gamma} w(s) \nabla_{\Gamma} w(s) dr d\theta \right) ds \\
&= \int_{\Gamma} \left(\int_{D_a(s)} \frac{1}{1 - \kappa(s)r \cos(\theta - \hat{\theta})} \delta\mathbb{C}_f \frac{d}{ds} w(s) \frac{d}{ds} w(s) dr d\theta \right) ds \\
&= \int_{\Gamma} \delta\mathbb{C}_f \nabla_{\Gamma} w(s) \nabla_{\Gamma} w(s) \underbrace{\left(\int_{D_a(s)} \frac{1}{1 - \kappa(s)r \cos(\theta - \hat{\theta})} dr d\theta \right)}_{=: g(s)\pi a^2} ds \\
&= (g\delta\mathbb{C}_f \nabla_{\Gamma} w, \nabla_{\Gamma} w)_{\Gamma}.
\end{aligned}$$

Where we define the function:

$$g(s) := \frac{1}{\pi a^2} \int_{D_a(s)} \frac{1}{1 - \kappa(s)r \cos(\theta - \hat{\theta})} dr d\theta.$$

□

Once g is computed, it is possible to compute the energy $(\delta\mathbb{C}_f \nabla Ew, \nabla Ew)_{\Omega_a}$ using a linear integration. In the case of a straight cylinder $\kappa(s) \equiv 0$, and we obtain again Equation 44.

The condition $r \leq a < \max_s 1/\kappa(s)$ is fundamental for the definition of g on the whole disk. Assume the curvature $\kappa(s)$ to be continuous, then $g(s)$ is continuous and there exist a constant $C_g > 0$ such that $g(s) \geq C_g > 0$.

To conclude, under the previous hypotheses on the domains, we introduce the extension operator:

$$\begin{aligned}
\bar{E}: H^1(\tilde{\Gamma}) &\rightarrow H^1(\tilde{\Omega}), \\
w &\rightarrow w \circ P_{\Gamma},
\end{aligned}$$

where P_{Γ} is the geometric projection from the domain $\tilde{\Omega}$ to $\tilde{\Gamma}$; for every $y \in \tilde{\Omega}$, $P_{\Gamma}y$ is the element of $\tilde{\Gamma}$ such that:

$$\text{dist}(y, P_{\Gamma}y) \leq \text{dist}(y, x) \quad \text{for every } x \in \tilde{\Gamma}.$$

As a consequence of our hypotheses on the fiber, for every $x \in \tilde{\Omega}$, we have $x \in D_a(P_{\Gamma}(x))$.

The operator \bar{E} is clearly bounded in L^2 , to prove it is bounded in H^1 we can use a strategy analogous to the one used in the proof of Proposition 3.3.

3.5. Modellistic Hypotheses

After proving that the average operator is continuous, we can finally describe the modellistic hypotheses we make on our model.

First modellistic hypothesis: fixed radius. We assume the fiber's radius a to remain constant. This implies that the fiber displacement w is an element of \hat{W} , where:

$$\hat{W} := \{w \in W : \text{for a.e. } x \in \Gamma, \bar{E}\bar{w} = w \text{ a.e. on } D_a(x)\}. \quad (46)$$

It is useful to introduce the space of functions of V which, restricted to Ω_a , belong to \hat{W} :

$$\hat{V} := \{v \in V : v|_{\Omega_a} \in \hat{W}\}.$$

Given $\hat{w} \in \hat{W}$, Equation 46 suggests the introduction of the following space:

$$W_\Gamma := (H_{0,B^e}^1(\Gamma))^d. \quad (47)$$

The following Proposition is an immediate consequence of the choice of our spaces:

Proposition 3.4. *The spaces W_Γ and \hat{W} are isomorphic.*

Second modellistic hypothesis: average non-slip condition. Consider $u \in V$ and $w \in W_\Gamma$, it is well known that in the case of thin fiber it is not possible to consider the classic non-slip condition:

$$u|_\Gamma = w.$$

With the results of Section 3.3 we can formulate following **average non-slip** condition:

$$\bar{u} = w. \quad (48)$$

As a second modellistic hypothesis we assume that the average non-slip condition can replace the non-slip condition.

As a justification, notice that when considering $w \in \hat{W}$, $u \in \hat{V}$, the classic non-slip condition, described in Equation 8, is equivalent to Equation 48. Moreover, with continuous function and a small radius a , the two conditions can be considered approximately the same.

3.6. Problem formulation

We assume the Modellistic Hypotheses described in the previous section hold:

- the fiber displacement w is contained in \hat{W} (we shall use W_Γ , since it is isomorphic to \hat{W}),
- we can impose the coupling between fibers and elastic matrix through the average non-slip condition .

This allows us to modify Problem 3 for the $3D - 1D$ case; the weak formulation of the average non-slip constraint on Γ is:

$$\langle q, \bar{u} - w \rangle = 0 \quad \forall q \in Q_\Gamma,$$

with $Q_\Gamma := H^{-1}(\Gamma)^d$.

For every $(u, w, q) \in V \times W_\Gamma \times Q_\Gamma$, we define the energy functional of our problem as:

$$\psi_T(u, w, \lambda) = \frac{1}{2}(\mathbb{C}_\Omega \nabla u, \nabla u)_\Omega + c_\Gamma(g\delta\mathbb{C}_f \nabla_\Gamma w, \nabla_\Gamma w)_\Gamma + (q, \bar{u} - w)_\Gamma - (b, u)_\Omega.$$

Then the saddle point problem becomes:

$$u, w, \lambda = \arg \inf_{\substack{u \in V \\ w \in W_\Gamma}} \left(\arg \sup_{\lambda \in Q_\Gamma} \psi_T(u, w, \lambda) \right). \quad (49)$$

Using the Euler-Lagrange equations as in Section 2.1, we obtain:

Problem 5 (1D-3D Weak Formulation). *Given $b \in L^2(\Omega)^d$, find $u \in V, w \in W_\Gamma, \lambda \in Q_\Gamma$ such that:*

$$\begin{aligned} (\mathbb{C}_\Omega \nabla u, \nabla v)_\Omega + \langle \lambda, \bar{v} \rangle &= (b, v)_\Omega & \forall v \in V, \\ c_\Gamma(g\delta\mathbb{C}_f \nabla_\Gamma w, \nabla_\Gamma y)_\Gamma - \langle \lambda, y \rangle &= 0 & \forall y \in W_\Gamma, \\ \langle q, \bar{u} - w \rangle &= 0 & \forall q \in Q_\Gamma. \end{aligned}$$

We now re-define the space $\mathbb{V} := V \times W_\Gamma$, and its norm: for every $(v, y) \in \mathbb{V}$, $\|(v, y)\|_{\mathbb{V}} := \|\cdot\|_V + \|\cdot\|_{W_\Gamma}$. We define the operators for the tubular fiber Ω_a :

$$\begin{aligned} \mathbb{F}_T &:= (\mathbb{C}_\Omega \nabla u, \nabla v)_\Omega + c_\Gamma(g\delta\mathbb{C}_f \nabla_\Gamma w, \nabla_\Gamma w)_\Gamma, \\ \mathbb{E}_T &:= \langle q, \bar{u} - w \rangle, \end{aligned}$$

obtaining a new saddle-point problem, which we study using the *inf* – *sup* conditions.

3.7. Well-posedness, existence and uniqueness

Similarly to the three-dimensional case, to prove the well-posedness and the existence and uniqueness of a solution we prove the following sufficient condition: there exist two positive constants $\alpha_5 > 0, \alpha_6 > 0$ such that

$$\begin{aligned} \inf_{q \in Q_\Gamma} \sup_{\mathbf{v} \in \mathbb{V}} \frac{\mathbb{E}(\mathbf{u}, q)}{\|\mathbf{u}\|_{\mathbb{V}} \|q\|_{Q_\Gamma}} &\geq \alpha_5 \\ \inf_{\mathbf{u} \in \ker \mathbb{E}} \sup_{\mathbf{v} \in \ker \mathbb{E}} \frac{\mathbb{F}(\mathbf{u}, \mathbf{v})}{\|\mathbf{u}\|_{\mathbb{V}} \|\mathbf{v}\|_{\mathbb{V}}} &\geq \alpha_6, \end{aligned}$$

Following a procedure similar to the one of Equation 20:

$$\begin{aligned} \ker \mathbb{E}_T &:= \{\mathbf{v} := (v, w) \in \mathbb{V} : \langle q, \bar{v} - y \rangle = 0 \ \forall q \in Q_\Gamma\} \\ &= \{\mathbf{v} := (v, w) \in \mathbb{V} : \bar{v} = w \text{ a.e. on } \Omega_a\}. \end{aligned}$$

With a variation on the proof of Proposition 3.2, it is possible to prove that there exists a positive constant $c_b > 0$, such that:

$$\bar{v} = w \text{ a.e. on } \Omega_a \Rightarrow \|w\|_\Gamma = \|\bar{v}\|_\Gamma \leq c_b \|v\|_{\Omega_a}$$

These conditions can be proved with the following Propositions:

Proposition 3.5. *There exists a constant $\alpha_5 > 0$ such that:*

$$\inf_{q \in Q_\Gamma} \sup_{(v,w) \in \mathbb{V}} \frac{\langle q, \bar{v} - w \rangle}{\|(v,w)\|_{\mathbb{V}} \|q\|_{Q_\Gamma}} \geq \alpha_5.$$

Moreover $\alpha_5 = 1$.

Proof. The non slip condition is given by the duality pairing between $Q_\Gamma = W'_\Gamma$ and W ; by definition of the norm in the dual space Q_Γ :

$$\begin{aligned} \|q\|_{Q_\Gamma} &= \sup_{w \in W_\Gamma} \frac{\langle q, w \rangle}{\|w\|_W} \\ &\leq \sup_{v \in V, w \in W_\Gamma} \frac{\langle q, \bar{v} - w \rangle}{(\|w\|_W^2 + \|v\|_V^2)^{\frac{1}{2}}}, \end{aligned}$$

where the last inequality can be proven fixing $v = 0$.

The final statement is found dividing by $\|q\|_{Q_\Gamma}$ and taking the $\inf_{q \in Q}$. \square

Proposition 3.6. *Assume \mathbb{C}_Ω and \mathbb{C}_f to be strongly elliptical, with constants c_Ω and c_f respectively such that $c_\Omega > c_f > 0$; there exists a constant $\alpha_6 > 0$ such that:*

$$\inf_{(u,w) \in \ker \mathbb{E}_T} \sup_{(v,y) \in \ker \mathbb{E}_T} \frac{(\mathbb{C}_\Omega \nabla v, \nabla u)_\Omega + c_\Gamma (g \delta \mathbb{C}_f \nabla_\Gamma y, \nabla_\Gamma w)_\Gamma}{\|(v,y)\|_{\mathbb{V}} \|(u,w)\|_{\mathbb{V}}} \geq \alpha_6.$$

Proof. For every $(u,w) \in \ker(\mathbb{E}_T)$:

$$\begin{aligned} &\sup_{(v,y) \in \ker(\mathbb{E}_T)} \frac{(\mathbb{C}_\Omega \nabla u, \nabla v)_\Omega + c_\Gamma (g \delta \mathbb{C}_f \nabla_\Gamma w, \nabla_\Gamma y)_\Gamma}{\|(v,y)\|_{\mathbb{V}}} \\ &\geq \frac{c_\Omega (\nabla u, \nabla u)_\Omega + c_\Gamma C_g (c_f - c_\Omega) (\nabla_\Gamma w, \nabla_\Gamma w)_\Gamma}{\|(u,w)\|_{\mathbb{V}}} \\ &\geq \frac{c_p c_\Gamma c_b \min(c_\Omega, C_g (c_f - c_\Omega))}{2} \frac{(u,u)_{H^1(\Omega)} + (w,w)_{H^1(\Gamma)}}{\|(u,w)\|_{\mathbb{V}}} \\ &\geq \alpha_6 \|(u,w)\|_{\mathbb{V}}, \end{aligned}$$

with $\alpha_6 := \frac{c_p c_\Gamma c_b \min(c_\Omega, C_g (c_f - c_\Omega))}{2}$.

The result is obtained dividing and considering the $\inf_{(u,w) \in \ker \mathbb{E}_T}$. \square

Using the saddle point theory we conclude that, under our modellistic assumptions, Problem 5 is well-posed, and has a unique solution.

3.8. Finite element discretization

The discretization of Problem 5 for thin fibers follows the steps of Section 2.3, on the domains Ω and Γ (the fiber's one-dimensional core). Consider two independent discretizations for these domains; the family $\mathcal{T}_h(\Omega)$ of regular meshes in Ω , and a family $\mathcal{T}_h(\Gamma)$ of regular meshes in Γ . We assume no geometrical error is committed when meshing. We consider two independent finite element discretizations $V_h \subset V$, $W_h \subset W_\Gamma$.

Similarly to the three-dimensional case, the duality pairing between Q_Γ and W_Γ can be represented using the L^2 scalar product in Γ :

$$\langle q, w \rangle = (q, w)_\Gamma.$$

Thus we discretize the duality pairing as the L^2 product, and consider $Q_h = W_h$. To handle the restriction of functions from V_h to W_h , we introduce the L^2 projection:

$$P_W: W_\Gamma \rightarrow W_h \subset L^2(\Gamma),$$

which is continuous: for every $w \in W_\Gamma$

$$\|P_W w\|_{L^2(\Gamma)} \leq \|w\|_\Gamma.$$

This condition is too weak for our Problem, which involves the gradient. We make the further assumption that the restriction $P_W|_{W_\Gamma} \neq 0$, and is H^1 -stable, i.e., there exists a positive constant c , such that for all $w \in W_\Gamma$:

$$\|\nabla_\Gamma P_W w\|_\Gamma \leq c \|\nabla_\Gamma w\|_\Gamma. \quad (50)$$

We assume that the H^1 -stability property holds uniformly on $\mathcal{T}_h(\Omega)$ and $\mathcal{T}_h(\Omega_f)$, provided that the mesh size h is comparable on the two domains.

We can now write the discretization of Problem 5:

Problem 6 (1D-3D Discretized Weak Formulation). *Given $b \in L^2(\Omega)^d$, find $u_h \in V_h, w_h \in W_h, \lambda_h \in Q_h$ such that:*

$$(\mathbb{C}_\Omega \nabla u_h, \nabla v_h)_\Omega + (\lambda_h, \bar{v}_h)_\Gamma = (b, v_h)_\Omega \quad \forall v_h \in V_h, \quad (51)$$

$$c_\Gamma (g \delta \mathbb{C}_f \nabla_\Gamma w_h, \nabla_\Gamma y_h)_\Gamma - (\lambda_h, y_h)_\Gamma = 0 \quad \forall y_h \in W_h, \quad (52)$$

$$(q_h, \bar{u}_h - w_h)_\Gamma = 0 \quad \forall q_h \in Q_h. \quad (53)$$

To study the saddle-point problem we define the Hilbert space $\mathbb{V}_h := V_h \times W_h$, with its norm, and the operators

$$\begin{aligned} \mathbb{F}_{T,h}: \mathbb{V}_h \times \mathbb{V}_h &\longrightarrow \mathbb{R} \\ (\mathbf{u}_h, \mathbf{v}_h) &\longmapsto (\mathbb{C}_\Omega \nabla u_h, \nabla v_h)_\Omega + c_\Gamma (g \delta \mathbb{C}_f \nabla_\Gamma w_h, \nabla_\Gamma y_h)_\Gamma, \end{aligned}$$

$$\begin{aligned} \mathbb{E}_{T,h}: \mathbb{V}_h \times Q_h &\longrightarrow \mathbb{R} \\ (\mathbf{u}_h, q_h) &\longmapsto (q_h, \bar{v}_h - w_h)_\Gamma. \end{aligned}$$

Then we can rewrite problem 6 in operatorial form, showing its saddle-point structure: find $\mathbf{u}_h \in \mathbb{V}_h, \lambda_h \in Q_h$ such that:

$$\begin{aligned} \mathbb{F}_{T,h}(\mathbf{u}_h, \mathbf{v}_h) + \mathbb{E}_{T,h}(\mathbf{v}_h, \lambda_h) &= (b, v_h)_\Omega & \forall \mathbf{v}_h := (v_h, y_h) \in \mathbb{V}_h \\ \mathbb{E}_{T,h}(q_h, \mathbf{u}_h) &= 0 & \forall q_h \in Q_h. \end{aligned}$$

Proposition 3.7. *There exists a constant $\alpha_7 > 0$, independent of h , such that:*

$$\inf_{q_h \in W_h} \sup_{(v_h, w_h) \in \mathbb{V}_h} \frac{(q_h, \bar{v}_h - w_h)_\Gamma}{\|(v_h, w_h)\|_{\mathbb{V}} \|q_h\|_\Gamma} \geq \alpha_7.$$

Proof. The proof is similar to the one of Proposition 2.3. For every $q_h \in Q_h$, by definition of the Q norm, representing the duality product as a scalar product in L^2 , there exists $\hat{w} \in W$ such that:

$$\|q_h\|_Q = \sup_{w \in W} \frac{(q_h, w)_\Gamma}{\|w\|_Q} = \frac{(q_h, \hat{w})_\Gamma}{\|\hat{w}\|_Q} = \frac{(q_h, P_W \hat{w})_\Gamma}{\|\hat{w}\|_Q}. \quad (54)$$

Using well-known properties of P_W , and the H^1 stability, we can prove there exists a c such that:

$$\|P_W \hat{w}\|_Q \leq c \|\hat{w}\|_Q.$$

Inserting this in Equation 54:

$$\begin{aligned} \|q_h\|_Q &\leq \frac{(q_h, P_W \hat{w})_\Gamma}{\|\hat{w}\|_Q} \leq c \frac{(q_h, P_W \hat{w})_\Gamma}{\|P_W \hat{w}\|_Q} \\ &\leq c \sup_{w_h \in W_h} \frac{(q_h, w_h)_\Gamma}{\|w_h\|_Q} \leq c \sup_{v_h \in V_h, w_h \in W_h} \frac{(q_h, v_h|_{\Omega_a} - w_h)_\Gamma}{(\|w_h\|_Q^2 + \|v_h\|_V^2)^{\frac{1}{2}}}, \end{aligned}$$

and we conclude as in Proposition 2.1. \square

To study the inf-sup condition for $\mathbb{F}_{T,h}$ define:

$$\begin{aligned} \ker(\mathbb{E}_{T,h}) &:= \{\mathbf{v}_h \in \mathbb{V}_h : (q_h, \bar{v}_h - w_h)_\Gamma = 0 \quad \forall q_h \in Q_h\} \\ &= \{\mathbf{v} \in \mathbb{V}_h : (q_h, \bar{v}_h)_\Gamma = (q_h, w_h)_\Gamma \quad \forall q_h \in Q_h\}. \end{aligned}$$

Proposition 3.8. *Assume \mathbb{C}_Ω and \mathbb{C}_f to be strongly elliptical, with constants c_Ω and c_f respectively such that $c_f > c_\Omega > 0$; then there exists a constant $\alpha_8 > 0$, independent of h , such that:*

$$\inf_{(u_h, w_h) \in \ker \mathbb{E}_{T,h}} \sup_{(v_h, y_h) \in \ker \mathbb{E}_{T,h}} \frac{(\mathbb{C}_\Omega \nabla v_h, \nabla u_h)_\Omega + c_\Gamma (g \delta \mathbb{C}_f \nabla_\Gamma y_h, \nabla_\Gamma w_h)_\Gamma}{\|(v_h, y_h)\|_{\mathbb{V}} \|(u_h, w_h)\|_{\mathbb{V}}} \geq \alpha_8.$$

Proof. The proof is almost identical to the one of Proposition 3.6. \square

One-Dimensional Approximation. The approach of Section 3 hides a computational difficulty: given $v_h \in V_h$, the average \bar{v}_h is obtained computing a number of two-dimensional integrals, nullifying the computational advantage of using one-dimensional fibers.

Since we are using finite element functions, there is a straight-forward solution to this problem: approximate \bar{v}_h with the restriction $v_h|_\Gamma$. This approximation is exact for every $v_h \in \hat{V}$, and can be justified by the fact that for every $v_h \in V_h$:

$$\lim_{a \rightarrow 0} \bar{v}_h(x) = v_h(x) \quad \text{for every } x \in \Gamma,$$

coherently with the initial choice of \bar{v}_h as a “substitute” of v_h .

While this approach simplifies our computations, it makes difficult the derivation of a formula for the error committed. The theoretical basis for such an estimate have been described in this paper, the estimate itself shall be the subject of future work.

4. Numerical validation

The analytical solution of Problems 3 and 5, even for simple configurations, is non-trivial: we chose some FRMs structures which are studied in literature, and used the known approximated solutions as a comparison for our model.

Using the deal.II library [3, 5, 39, 53], and the deal.II step-60 tutorial [35] we developed a model for thin fibers proposed in Section 3, and compared it with the Rule of Mixtures and the Halpin-Tsai configurations in some pull and push tests.

Numerical Setting. For our numerical solution, we now describe how to solve Problem 6 on a collection of fibers, while reducing the system size; we begin by redefining our spaces and meshes:

- Ω : the elastic matrix, on which we build the finite element space, of dimension $N \in \mathbb{N}$:

$$V_h = \text{span}\{v_i\}_{i=1}^N \subset H^1(\Omega).$$

- $\Gamma \subset \Omega$: the collection of $n_f \in \mathbb{N}$ fibers, i.e., $\Gamma := \bigcup_{k=1}^{n_f} \Gamma_k$, with the finite element discretization, of dimension $M \in \mathbb{N}$:

$$W_h = \text{span}\{w_a\}_{i=a}^M \subset H^1(\Gamma).$$

- Q_h : the space of the Lagrange multiplier, discretized using the same base of W_h .

We use i, j as indices for the space V_h and a, b as indices for the space W_h , and assume all hypotheses on spaces and meshes of section 3.8 are satisfied.

We assume that each fiber is parametrized by $X_k: I_k \rightarrow \Gamma_k$, where I_k is a finite interval in \mathbb{R} , and $1 \leq k \leq n_f$. We assume for any $1 \leq j < k \leq n_f$ we have $I_k \cap I_j = \emptyset$. Then we can define $X: \bigcup_{k=1}^{n_f} I_k \rightarrow \Gamma$, which parametrizes all fibers contained in Γ . For each fiber Γ_k we define its tubular neighborhood $\Omega_{a,k}$, and we define

$$\Omega_f := \bigcup_{k=1}^{n_f} \Omega_{a,k}.$$

We define the following sparse matrices:

$$\begin{aligned} A: V_h &\rightarrow V'_h & A_{ij} &:= (\mathbb{C}_\Omega \nabla v_i, \nabla v_j)_\Omega, \\ K: W_h &\rightarrow W'_h & K_{ab} &:= c_\Gamma (g \delta \mathbb{C}_f \nabla_\Gamma w_a, \nabla_\Gamma w_b)_\Gamma, \\ B: V_h &\rightarrow Q'_h & B_{ia} &:= (v_i|_\Gamma, w_a)_\Gamma = (v_i \circ X, w_a)_\Gamma, \\ L: W_h &\rightarrow Q'_h & L_{ab} &:= (w_a, w_b)_\Gamma. \end{aligned} \tag{55}$$

Here B is the coupling matrix from V_h to W_h , M the mass-matrix of W_h .

After defining the vector $g_i := (b, v_i)_\Omega$, Problem 6 can be expressed in matrix form as: find $(u, w, \lambda_h) \in V_h \times W_h \times Q_h$ such that

$$\begin{pmatrix} A & 0 & B^T \\ 0 & K & -L^T \\ B & -L & 0 \end{pmatrix} \begin{pmatrix} u \\ w \\ \lambda \end{pmatrix} = \begin{pmatrix} g \\ 0 \\ 0 \end{pmatrix}. \tag{56}$$

This system has size NM^2 : computationally it is convenient to reduce its size. From the second line of the Block Matrix 56:

$$Kw = L^T \lambda = L\lambda \Rightarrow \lambda = L^{-1}Kw.$$

System 56 becomes:

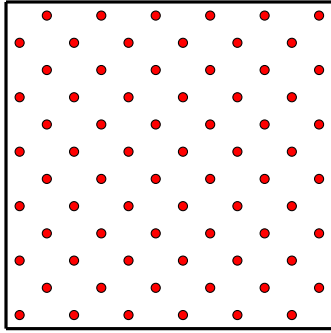
$$\begin{pmatrix} A & B^T L^{-1} K \\ B & -L \end{pmatrix} \begin{pmatrix} u \\ w \end{pmatrix} = \begin{pmatrix} g \\ 0 \end{pmatrix}. \quad (57)$$

We remove w using the equation $Bu = Lw \Rightarrow w = L^{-1}Bu$ and obtaining:

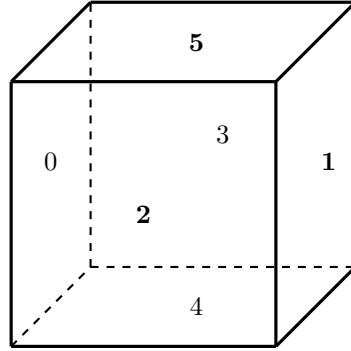
$$(A + B^T L^{-1} K L^{-1} B)u = (A + P_\Gamma^T K P_\Gamma)u = g, \quad (58)$$

where $P_\Gamma := L^{-1}B$. Boundary conditions are imposed weakly, using Nitsche method (as in [50]).

4.1. Model description



(a) Section with homogeneous fibers.



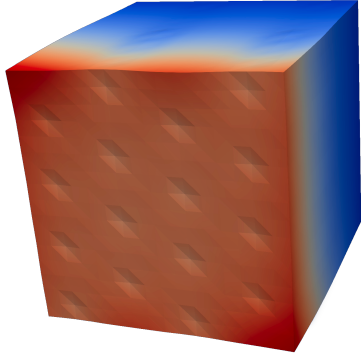
(b) Ω 's faces numbering

The elastic matrix we consider in our tests is the unitary cube $\Omega := [0, 1]^3$. All considered meshes are only uniformly refined hexaedral meshes, and we use only linear finite elements.

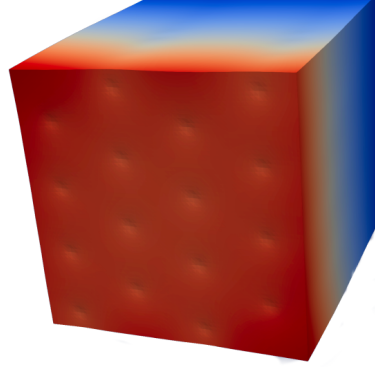
The elastic tensors used are described in Equations 23 – 25; for the model description we use the following parameters:

- r_Ω : global refinements of the Ω mesh.
- r_Γ : global refinements of the Γ mesh.
- $\lambda_\Omega, \mu_\Omega$: Lamé parameters for the elastic matrix.
- λ_f, μ_f : Lamé parameters for the fibers.
- β : fiber volume ratio or representative volume element (RVE), i.e., $\beta = |\Omega_f|/|\Omega|$.
- a : the radius of the fibers.

For the boundary conditions we refer to Figure 5b.



(a) Pull test example, with $r_\Omega = 4$



(b) Pull test example, with $r_\Omega = 6$

4.2. Homogeneous fibers

In our first test we consider a unidirectional composite, where fibers are uniform in properties and diameter, continuous, and parallel throughout the composite Ω (see Figure 5a).

We compare the results obtained with our model with the ones obtained using the Rule of Mixtures [20, 2], which agrees with experimental tests especially for tensile loads, and when the fiber ratio β is small.

The composite stress-strain equation, under the condition $u|_{\Omega_f} = w$, is:

$$S[u, w] = \frac{1}{2}(\mathbb{C}_\Omega Eu, Eu)_\Omega + \frac{1}{2}(g\delta\mathbb{C}_f Ew, Ew)_{\Omega_f}.$$

Using the Rule of Mixtures we can approximate the integral over Ω_a with one over Ω :

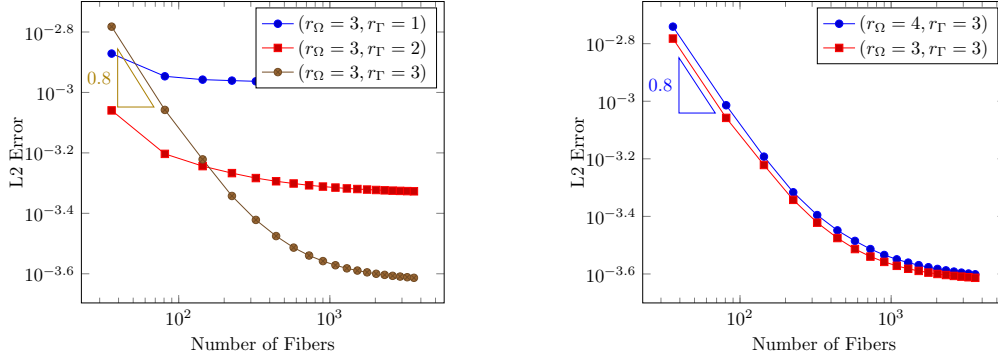
$$(\delta\mathbb{C}_f Ew, Ew)_{\Omega_f} \approx \beta(\delta\mathbb{C}_f Eu, Eu)_\Omega,$$

obtaining:

$$S[u] = \frac{1}{2}(\mathbb{C}_\Omega Eu, Eu)_\Omega + \beta\frac{1}{2}(\delta\mathbb{C}_f Eu, Eu)_\Omega. \quad (59)$$

Multiple tests were run, keeping β constant, while increasing the fiber density and reducing the fiber diameter; we expect this process to render the coupled model solution increasingly close to the homogenized one.

Comparing solutions. Figures 6a and 6b illustrate the influence of Ω 's refinement on the final result, when using few fibers on a pull test. Stiff fibers oppose being stretched, deforming the elastic matrix Ω through the non-slip condition: near each fiber, the deformation of Ω should be symmetrical, resembling a cone. This effect is better described in Figure 6b, where the higher value of r_Ω results in greater geometrical flexibility of the elastic matrix, allowing a better description of the effect of each fiber. Lower values of r_Ω result in a non symmetrical solution, as in Figure 6a. The lower geometrical



(a) Pull Test, $\lambda = \lambda_F = 0.4, \mu = 1,$
 $\mu_F = 1000, \beta = 0.1.$

(b) Pull Test, $\lambda = \lambda_F = 0.4, \mu = 1,$
 $\mu_F = 1000, r_\Omega = 3, r_\Gamma = 3.$

Figure 7: Pull tests with varying refinements.

flexibility results in an “averaged” solution which, in the case of few fibers, is closer to the homogenized model.

To describe the slope in the plots, let $\mathbf{e}_1, \mathbf{e}_2$ be the L^2 errors and $n_{f,1}, n_{f,2}$ are the fiber numbers for two subsequent simulations; to compute the slope we then apply the formula:

$$\frac{\ln(\mathbf{e}_2/\mathbf{e}_1)}{\ln(n_{f,2}/n_{f,1})}.$$

Pull test along fibers. Dirichlet homogeneous conditions is applied to face 0, Neumann homogeneous conditions is applied to faces 2, 3, 4, 5. In the Push Test, the Neumann condition 0.05 is applied to face 1. For the Pull Test, the value -0.05 is applied to the same face. Boundary conditions are applied only to $\partial\Omega$; the fibers interact through the coupling with the elastic matrix.

We report here only data from pull tests, as push tests gave comparable results.

The use of the projection matrix $P_\Gamma: V_h \rightarrow W_h$, and the error estimate for the fully three-dimensional case (Inequality 31), both suggest that the solution quality on the elastic matrix depends on both V_h and W_h . This is apparent in Figure 7a, where for $r_\Gamma = 1$ the mesh of Γ is unable to describe the stretch of the material, resulting in the error remaining approximately constant after a certain fiber density is reached. A similar behaviour emerges in the case $r_\Gamma = 2$.

In a similar manner Figure 7b shows that refining only the elastic matrix does not improve the solution quality: as the number of fibers increases, the error converges to approximately the same value, which is limited by r_Γ .

Figure 8 shows an error comparison as the value of μ_F varies: as expected our model is better suited for stiff fibers.

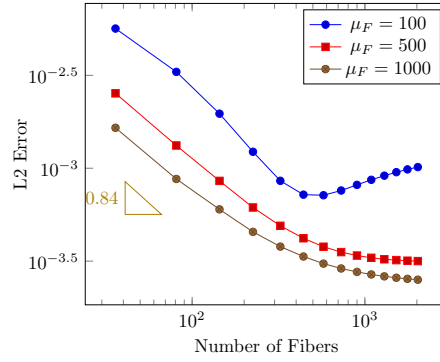


Figure 8: Pull Test with varying μ_F , $\lambda = \lambda_F = 0.4$, $\mu = 1$, $\beta = 0.1$, $r_\Omega = 3$, $r_\Gamma = 3$

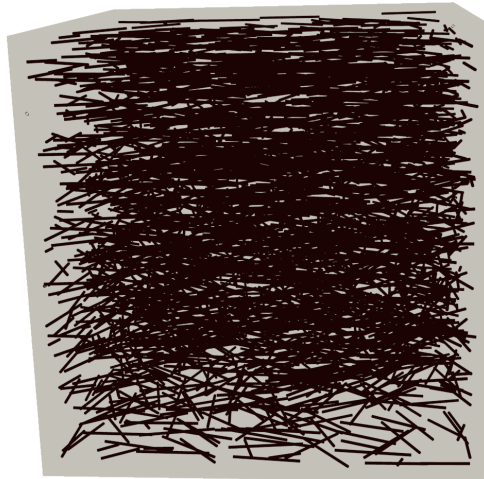


Figure 9: Random Fibers Disposition

4.3. Random fibers

Our second test is a pull test on a more complex model: a random chopped fiber reinforced composite.

We distribute small fibers at a random point of Ω , with a random direction parallel to the $\langle x, y \rangle$ plane; the fibers share the same size and properties. If a fiber surpasses the edge of Ω , it is cut.

For more details on the algorithm used to distribute the fibers see the Random Sequential Adsorption algorithm [46]; our implementation generates only the plane angle, and does not implement an intersection-avoidance mechanism.

As a comparison model, we estimate the material parameters using the empirical Halpin-Tsai [19]; which we report here for longitudinal moduli, as described in [2]. The fibers have length l , diameter d , the fiber and the matrix Young moduli are E_f and E_m respectively, β is the volume fraction occupied by the fibers.

We define two empirical constants:

$$\eta_L = \frac{(E_f/E_m) - 1}{(E_f/E_m) + (2l/d)}, \quad (60)$$

$$\eta_T = \frac{(E_f/E_m) - 1}{(E_f/E_m) + 2}. \quad (61)$$

This allows to compute the longitudinal and transverse moduli for aligned short fibers:

$$E_L = \frac{1 + (2l/d)\eta_L\beta}{1 - \eta_L\beta}, \quad (62)$$

$$E_T = \frac{1 + 2\eta_T\beta}{1 - \eta_T\beta}. \quad (63)$$

If fibers are randomly oriented in a plane the following equations can be used to predict the elastic modulus:

$$E_C = \frac{3}{8}E_L + \frac{5}{8}E_T, \quad (64)$$

$$\mu_C = \frac{1}{8}E_L + \frac{1}{4}E_T. \quad (65)$$

Since a random fiber composite is considered isotropic in its plane, the Poisson's ratio can be calculated as:

$$\nu_R = \frac{E_C}{2\mu_C} - 1. \quad (66)$$

The properties of this composite do not depend directly on the fiber length or radius, but on the aspect ratio l/d .

Our test setting runs on the unitary cube, with a fiber ratio $\beta = 0.135$ and a fiber aspect ratio of $\frac{l}{2r} \approx 10$, where l is the fiber's length and r is the fiber's radius; the values used are described in Table 1.

We could not find an exact estimate of the error convergence, but we expect the solution to improve as the number of fibers increases because:

Fiber length	0.6	0.4	0.3	0.25	0.225	0.2	0.18
Fiber radius	0.03	0.02	0.015	0.0125	0.01125	0.01	0.009
Number of Fibers	79	268	637	1100	1509	2149	2947

Table 1: Fiber Parameters

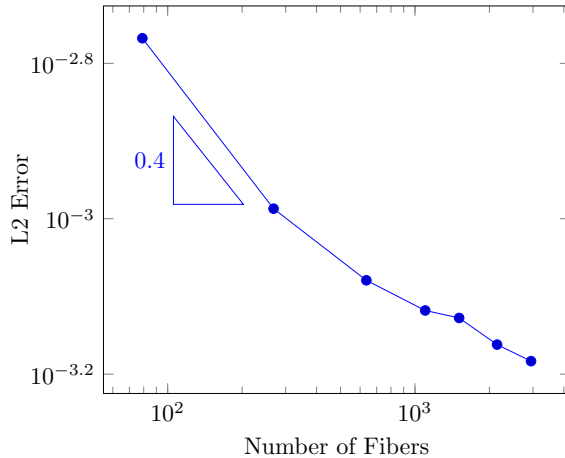


Figure 10: Random Pull Test with one dimensional approximation; global refinement of Ω : 4, global refinement of Γ : 2.

- the fiber radius a reduces, improving of the average non-slip condition,
- more fibers result in a more homogeneous material on the planes parallel to the $\langle x, y \rangle$ plane.

Following [46], we consider a short fiber E-glass/urethane composite: the fiber and matrix Young's modulus are, respectively, $E_f = 70GPa$ and $E_m = 3GPa$, while the Poisson ratios are $\nu_f = 0.2$ and $\nu_m = 0.38$. These values were converted to the Lamé parameters using the classic formulas for hyper elastic materials.

The predicted parameters for the composite are: $E_C = 2.20GPa$ and $\nu_C = 0.38GPa$; these are slightly different from [46] because, in the Halpin-Tsai equations, l/d was used instead of $2l/d$. The boundary conditions used for the pull tests are the same of Paragraph 4.2.

We limit the global refinements of Γ , in order to obtain cells of approximately the same size on both Ω and the fibers. The results are shown in Figure 10: as the number of fiber increases the error reduces, but because the random fiber model is more complex than the homogeneous one, the final error achieved is higher than the one reached in the previous test.

5. Conclusions

Starting from a linearly elastic description of bi-phasic materials, we derive a new formulation for fiber reinforced materials where independent meshes are used to discretize the fibers and the elastic matrix, and the coupling between the two phases is obtained via a distributed Lagrange multiplier.

We prove existence and uniqueness of a solution for the final saddle point problem, and we analyze a simplified model where fibers are discretised as one-dimensional.

The model is validated against the Rule of Mixtures and the Hapin-Tsai equations, where we test our discretisation with uniform and random distributions of fibers. The true benefit of our model, however, lies in the possibility to tackle complex and intricate fiber structures independently from the background elastic matrix discretization, opening the way to the efficient simulation of complex multi-phase materials.

From the numerical analysis point of view, there are some issues that deserve further development, such as studying the effects of the operator B on the final error, finding better preconditioners for the final system, and exploring different coupling operators for the one dimensional coupling operator.

The formulation of our method makes it particularly suited for extensions to more complex situations, e.g., three-phasic materials, or materials where no-slip is replaced by other, more realistic conditions.

Acknowledgements

The authors would like to thank Prof. Lucia Gastaldi, for the fruitful conversations and suggestions that greatly improved this manuscript, and to thank Dr. Giovanni Noselli, and Maicol Caponi for their priceless suggestions and insights in their fields of expertise.

Bibliography

- [1] D. F. Adams and D. R. Doner. Transverse normal loading of a unidirectional composite. *Journal of composite Materials*, 1(2):152–164, 1967.
- [2] B. D. Agarwal, L. J. Broutman, and K. Chandrashekhara. *Analysis and performance of fiber composites*. John Wiley & Sons, 2017.
- [3] G. Alzetta, D. Arndt, W. Bangerth, V. Boddu, B. Brands, D. Davydov, R. Gassmoeller, T. Heister, L. Heltai, K. Kormann, M. Kronbichler, M. Maier, J.-P. Pelteret, B. Turcksin, and D. Wells. The deal.II library, version 9.0. *Journal of Numerical Mathematics*, 26(4):173–183, 2018.
- [4] F. Auricchio, D. Boffi, L. Gastaldi, A. Lefieux, and A. Reali. On a fictitious domain method with distributed lagrange multiplier for interface problems. *Applied Numerical Mathematics*, 95:36–50, 2015.
- [5] W. Bangerth, R. Hartmann, and G. Kanschat. deal.II – a general purpose object oriented finite element library. *ACM Trans. Math. Softw.*, 33(4):24/1–24/27, 2007.
- [6] R. Barrage, S. Potapenko, and M. A. Polak. Modelling transversely isotropic fiber-reinforced composites with unidirectional fibers and microstructure. *Mathematics and Mechanics of Solids*, page 1081286519838603, 2019.
- [7] T. Behzad and M. Sain. Finite element modeling of polymer curing in natural fiber reinforced composites. *Composites Science and Technology*, 67(7-8):1666–1673, 2007.
- [8] D. Boffi, F. Brezzi, M. Fortin, et al. *Mixed finite element methods and applications*, volume 44. Springer, 2013.
- [9] D. Boffi and L. Gastaldi. A finite element approach for the immersed boundary method. *Computers & structures*, 81(8-11):491–501, 2003.

- [10] D. Boffi and L. Gastaldi. A fictitious domain approach with lagrange multiplier for fluid-structure interactions. *Numerische Mathematik*, 135(3):711–732, 2017.
- [11] D. Boffi, L. Gastaldi, L. Heltai, and C. S. Peskin. On the hyper-elastic formulation of the immersed boundary method. *Computer Methods in Applied Mechanics and Engineering*, 197(25-28):2210–2231, 2008.
- [12] D. Boffi, L. Gastaldi, and M. Ruggeri. Mixed formulation for interface problems with distributed lagrange multiplier. *Computers & Mathematics with Applications*, 68(12):2151–2166, 2014.
- [13] W. D. Callister, D. G. Rethwisch, et al. *Materials science and engineering: an introduction*, volume 7. John Wiley & Sons New York, 2007.
- [14] C. D’Angelo. Finite element approximation of elliptic problems with dirac measure terms in weighted spaces: applications to one-and three-dimensional coupled problems. *SIAM Journal on Numerical Analysis*, 50(1):194–215, 2012.
- [15] C. D’Angelo and A. Quarteroni. On the coupling of 1d and 3d diffusion-reaction equations: application to tissue perfusion problems. *Mathematical Models and Methods in Applied Sciences*, 18(08):1481–1504, 2008.
- [16] J. J. Duistermaat and J. A. Kolk. *Multidimensional real analysis I: differentiation*, volume 86. Cambridge University Press, 2004.
- [17] K. S. Eloh, A. Jacques, and S. Berbenni. Development of a new consistent discrete green operator for fft-based methods to solve heterogeneous problems with eigenstrains. *International Journal of Plasticity*, 116:1–23, 2019.
- [18] M. E. Gurtin. *An Introduction to Continuum Mechanics*. Mathematics in Science and Engineering 158. Academic Press, 1981.
- [19] J. C. Halpin and J. Kardos. The halpin-tsai equations: a review. *Polymer engineering and science*, 16(5):344–352, 1976.
- [20] Z. Hashin. On elastic behaviour of fibre reinforced materials of arbitrary transverse phase geometry. *Journal of the Mechanics and Physics of Solids*, 13(3):119–134, 1965.
- [21] Z. Hashin. *Theory of fiber reinforced materials*. NASA, Washington, United States, 1972.
- [22] Z. Hashin. Analysis of composite materials—a survey. *Journal of Applied Mechanics*, 50(3):481–505, 1983.
- [23] L. Heltai. On the stability of the finite element immersed boundary method. *Computers & Structures*, 86(7-8):598–617, 2008.
- [24] L. Heltai and A. Caiazzo. Multiscale modeling of vascularized tissues via non-matching immersed methods. *International Journal for Numerical Methods in Biomedical Engineering*, 2019. In press.
- [25] L. Heltai and F. Costanzo. Variational implementation of immersed finite element methods. *Computer Methods in Applied Mechanics and Engineering*, 229-232, 2012.
- [26] L. Heltai and N. Rotundo. Error estimates in weighted sobolev norms for finite element immersed interface methods. *Computers and Mathematics with Applications*, 2019. In press.
- [27] G. A. Holzapfel et al. Biomechanics of soft tissue. *The handbook of materials behavior models*, 3:1049–1063, 2001.
- [28] G. A. Holzapfel and T. C. Gasser. A viscoelastic model for fiber-reinforced composites at finite strains: Continuum basis, computational aspects and applications. *Computer methods in applied mechanics and engineering*, 190(34):4379–4403, 2001.
- [29] G. A. Holzapfel, T. C. Gasser, and R. W. Ogden. A new constitutive framework for arterial wall mechanics and a comparative study of material models. *Journal of elasticity and the physical science of solids*, 61(1-3):1–48, 2000.
- [30] P. A. Huijing. Muscle as a collagen fiber reinforced composite: a review of force transmission in muscle and whole limb. *Journal of biomechanics*, 32(4):329–345, 1999.
- [31] K. Iizuka, M. Ueda, T. Takahashi, A. Yoshimura, and M. Nakayama. Development of a three-dimensional finite element model for a unidirectional carbon fiber reinforced plastic based on x-ray computed tomography images and the numerical simulation on compression. *Advanced Composite Materials*, 28(1):73–85, 2019.
- [32] T. Konopczyński, D. Rathore, J. Rathore, T. Kröger, L. Zheng, C. S. Garbe, S. Carmignato, and J. Hesser. Fully convolutional deep network architectures for automatic short glass fiber semantic segmentation from ct scans. *arXiv preprint arXiv:1901.01211*, 2019.
- [33] E. Kreyszig. *Differential geometry*. University of Toronto Press, 1963.
- [34] S. K. Kyriacou, J. D. Humphrey, and C. Schwab. Finite element analysis of nonlinear orthotropic hyperelastic membranes. *Computational Mechanics*, 18(4):269–278, Jul 1996.
- [35] G. A. L. Heltai. The deal.ii tutorial step-60: non-matching grid constraints through distributed lagrange multipliers. 2018.

- [36] S.-Y. Lee. *Accelerator physics*. World scientific publishing, 2018.
- [37] Z. Lu, Z. Yuan, and Q. Liu. 3d numerical simulation for the elastic properties of random fiber composites with a wide range of fiber aspect ratios. *Computational Materials Science*, 90:123–129, 2014.
- [38] V. Lucas, J.-C. Golinval, S. Paquay, V.-D. Nguyen, L. Noels, and L. Wu. A stochastic computational multiscale approach; application to mems resonators. *Computer Methods in Applied Mechanics and Engineering*, 294:141–167, 2015.
- [39] M. Maier, M. Bardelloni, and L. Heltai. `LinearOperator` – a generic, high-level expression syntax for linear algebra. *Computers and Mathematics with Applications*, 72(1):1–24, 2016.
- [40] P. K. Mallick. *Fiber-reinforced composites: materials, manufacturing, and design*. CRC press, 2007.
- [41] J. E. Marsden and T. J. Hughes. *Mathematical foundations of elasticity*. Courier Corporation, 1994.
- [42] P. K. Mehta. *Concrete. Structure, properties and materials*. McGraw-Hill, 1986.
- [43] H. Moulinec and P. Suquet. A numerical method for computing the overall response of nonlinear composites with complex microstructure. *Computer methods in applied mechanics and engineering*, 157(1-2):69–94, 1998.
- [44] H. Moulinec and P. Suquet. Comparison of fft-based methods for computing the response of composites with highly contrasted mechanical properties. *Physica B: Condensed Matter*, 338(1-4):58–60, 2003.
- [45] T. Nakamura and S. Suresh. Effects of thermal residual stresses and fiber packing on deformation of metal-matrix composites. *Acta metallurgica et materialia*, 41(6):1665–1681, 1993.
- [46] Y. Pan, L. Iorga, and A. A. Pelegri. Analysis of 3d random chopped fiber reinforced composites using fem and random sequential adsorption. *Computational Materials Science*, 43(3):450–461, 2008.
- [47] C. S. Peskin. The immersed boundary method. *Acta Numerica*, 11(1):479–517, jan 2002.
- [48] K. L. Pickering, M. A. Efendy, and T. M. Le. A review of recent developments in natural fibre composites and their mechanical performance. *Composites Part A: Applied Science and Manufacturing*, 83:98–112, 2016.
- [49] A. C. Pipkin. Integration of an equation in membrane theory. *Zeitschrift für angewandte Mathematik und Physik ZAMP*, 19(5):818–819, Sep 1968.
- [50] N. Rotundo, T.-Y. Kim, W. Jiang, L. Heltai, and E. Fried. Error analysis of a b-spline based finite-element method for modeling wind-driven ocean circulation. *Journal of Scientific Computing*, 69(1):430–459, 2016.
- [51] S. Roy, L. Heltai, and F. Costanzo. Benchmarking the immersed finite element method for fluid-structure interaction problems. *Computers and Mathematics with Applications*, 69:1167–1188, 2015.
- [52] E. Ryder. *Nonlinear guided waves in fibre optics*. 1993.
- [53] A. Sartori, N. Giuliani, M. Bardelloni, and L. Heltai. `deal2lkit`: A toolkit library for high performance programming in deal.II. *SoftwareX*, 7:318–327, 2018.
- [54] C. Tang. An orthogonal coordinate system for curved pipes (correspondence). *IEEE Transactions on Microwave Theory and Techniques*, 18(1):69–69, 1970.
- [55] A. Zaoui. Continuum micromechanics: survey. *Journal of Engineering Mechanics*, 128(8):808–816, 2002.